Experimental Neurology 311 (2019) 15–32

Contents lists available at ScienceDirect

Experimental Neurology

journal homepage: www.elsevier.com/locate/yexnr

Research Paper

Mesenchymal stem cells-derived IL-6 activates AMPK/mTOR signaling to inhibit the proliferation of reactive astrocytes induced by hypoxic-ischemic brain damage

Mulan He[a,b,c,d], Xia Shi[a,b,c,d], Miao Yang[a,b,c,d], Ting Yang[a,b,c], Tingyu Li[a,b,c], Jie Chen[a,b,c,d,*]

[a] Children's Nutrition Research Center, Children's Hospital of Chongqing Medical University, Chongqing 400014, China
[b] Ministry of Education Key Laboratory of Child Development and Disorders, Children's Hospital of Chongqing Medical University, Chongqing 400014, China
[c] China International Science and Technology Cooperation Base of Child Development and Critical Disorders, Chongqing 400014, China
[d] Chongqing Stem Cell Therapy Engineering Technical Center, Children's Hospital of Chongqing Medical University, Chongqing 400014, China

ARTICLE INFO

Keywords:
Astrocyte proliferation
Interleukin-6
Mammalian AMP-activated protein kinaseα
Mammalian target of rapamycin
Mesenchymal stem cells
Hypoxic-ischemic brain damage

ABSTRACT

Mesenchymal stem cells (MSCs) treatment is an effective strategy for the functional repair of central nervous system (CNS) insults through the production of bioactive molecules. We have previously demonstrated that the interleukin-6 (IL-6) secreted by MSCs plays an anti-apoptotic role in injured astrocytes and partly promotes functional recovery in neonatal rats with hypoxic-ischemic brain damage (HIBD). However, the mechanisms of IL-6 underlying the proliferation of injured astrocytes have not been fully elucidated. In this study, we investigated the therapeutic effects of MSCs on astrocyte proliferation in neonatal rats subjected to HIBD. A HIBD model was established in Sprague Dawley (SD) rats, and MSCs were administered by intracerebroventricular injection 5 days after HIBD. Rat primary astrocytes were cultured, subjected to oxygen glucose deprivation (OGD) injury and then immediately co-cultured with MSCs *in vitro*. Immunofluorescence staining, Cell Counting Kit (CCK)-8, flow cytometry, Ca^{2+} imaging, enzyme-linked immunosorbent assay (ELISA), western blotting, and co-immunoprecipitation (Co-IP) were performed. We found that MSCs transplantation not only promoted the recovery of learning and memory function in HIBD rats but also significantly reduced the number of $Ki67^{+}$/glial fibrillary acidic protein $(GFAP)^{+}$ cells in the hippocampi 7–14 days after HIBD. In addition to increasing IL-6 expression in both the hippocampi of HIBD rats and astrocyte culture medium, MSCs treatment *in vitro* significantly increased the expression levels of glycoprotein (gp) 130 and phosphorylated AMP-activated protein kinase α (p-AMPKα) and decreased the expression levels of p-mammalian target of rapamycin (mTOR) and its downstream targets. Furthermore, MSCs treatment induced a protein-protein interaction between gp130 and p-AMPKα. Suppression of IL-6 expression in MSCs reversed the above regulatory functions of MSCs in hippocampal astrocytes. The utilization of rapamycin further confirmed that mTOR participated in the proliferation of reactive astrocytes. These findings suggest that endogenous IL-6 produced by MSCs in the HIBD microenvironment provides therapeutic advantages by activating AMPK/mTOR signaling, thus reducing the proliferation of reactive astrocytes.

Abbreviations: MSCs, mesenchymal stem cells; IL-6, interleukin-6; OGD, oxygen and glucose deprivation; HIBD, hypoxic-ischemic brain damage; p-mTOR, phospho-mammalian target of rapamycin; p-AMPK, phospho-mammalian AMP-activated protein kinase; p70S6K, p70 ribosomal S6 kinase; 4E-BPs, eIF4E binding proteins; TBI, traumatic brain injury; GFAP, glial fibrillary acidic protein; IL-6Rα, interleukin-6 α receptor; gp130, glycoprotein 130; siRNA, small interfering RNA; Co-IP, co-immunoprecipitation; MCAO, middle cerebral artery occlusion; DG, dentate gyrus; SD rats, Sprague Dawley rats; SPF, specific pathogen-free; DMSO, dimethyl sulfoxide; PBS, phosphate-buffered saline; FBS, fetal bovine serum; DAPI, 4′,6-diamidino-2-phenylindole; ELISA, enzyme-linked immunosorbent assay; BSA, bovine serum albumin; SDS-PAGE, sodium dodecyl sulfate-polyacrylamide gel electrophoresis; HBSS, HEPES-buffered Hank's Balanced Salt Solution; CCK-8, Cell Counting Kit-8; EDTA, ethylenediaminetetraacetic acid; SEM, standard error of the mean; ANOVA, one-way analysis of variance; pMCAO, permanent middle cerebral artery occlusion; NF-κB, nuclear factor kappa-light-chain-enhancer of activated B cells; EAE, experimental autoimmune encephalomyelitis (EAE); ALS, amyotrophic lateral sclerosis

* Corresponding author at: Children's Nutrition Research Center, Children's Hospital of Chongqing Medical University, Chongqing 400014, China.
E-mail address: jchen010@hospital.cqmu.edu.cn (J. Chen).

https://doi.org/10.1016/j.expneurol.2018.09.006
Received 27 April 2018; Received in revised form 10 August 2018; Accepted 7 September 2018
Available online 10 September 2018
0014-4886/

1. Introduction

Hypoxic-ischemic brain damage (HIBD) often leads to permanent brain damage in human neonates, resulting in nervous system disability or even infantile mortality (Yasuhara et al., 2006). Currently, hypothermia treatment is the only available treatment that is known to be effective in improving the outcome of neonatal HIBD (Yenari et al., 2008; Shankaran et al., 2002). However, hypothermia (HT) for neonatal HIBD is advised to start within the first 6 h after birth (Sabir et al., 2012). The therapeutic time window of hypothermia for neonatal HIBD is quite narrow. Therefore, the development of new, safe, and effective additional treatments besides therapeutic hypothermia, to enhance neuroprotective effects is an urgent requirement. The treatment of neonatal animal models of HIBD with mesenchymal stem cells (MSCs) can effectively decrease the injured area and improve functional outcomes (van Velthoven et al., 2010a, 2011). The mechanisms by which MSCs transplantation provides therapeutic benefits remain unclear. One major postulated mechanism involves the secretion of neurotrophic and growth factors to provide a microenvironment conducive to injury restoration (Qu et al., 2007; van Velthoven et al., 2011). Our previous study also demonstrated that MSCs can suppress the apoptosis of astrocytes injured by oxygen and glucose deprivation (OGD) *in vitro via* endogenous interleukin-6 (IL-6) secretion, thus exerting neuroprotective effects (Gu et al., 2016).

Astrocytes are among the most abundant cells in the mammalian central nervous system (CNS) and perform various biological functions in healthy CNS, including providing structural and metabolic support for neurons, regulating the extracellular ion environment, and removing excessive neurotransmitters (Sofroniew, 2009). In addition, astrocytes participate in recovery after neurological diseases such as stroke, traumatic brain injury (TBI), Alzheimer's disease, and Parkinson's disease (Verkhratsky et al., 2012). After brain injury, including HIBD, the proliferation rate of astrocytes accelerates, accompanied by the elevated expression of glial fibrillary acidic protein (GFAP) and cell hypertrophy to form “reactive” astrocytes (Pekny and Nilsson, 2005; Sofroniew, 2009). Reactive astrocytes are believed to have both positive and negative effects. Persistent proliferation or even glial scar formation obstructs neuronal axonal regeneration and communication, thus preventing restoration following CNS damage (Gadient and Otten, 1997; Pekny and Nilsson, 2005; Pekny and Pekna, 2014). The attenuation of astrocyte proliferation at the subacute stage is beneficial for facilitating functional repair following damage, for example, from brain hypoxia and brain trauma (Zhu et al., 2007a).

IL-6 is an important mediator involved in the regulation of cell proliferation, differentiation, survival, and apoptosis through the activation of target genes (Heinrich et al., 2003). IL-6 exerts its action *via* the signal transduction receptor glycoprotein (gp) 130, which is the core receptor of IL-6, to activate its downstream signaling pathways (Heinrich et al., 2003). Mammalian AMP-activated protein kinase α (AMPKα), a switch that controls metabolism, has been confirmed to be a downstream target of IL-6, and its activation suppresses mammalian target of rapamycin (mTOR) signaling to inhibit protein synthesis (Winder, 2001; Laplante and Sabatini, 2012). mTOR is an evolutionarily conserved serine/threonine kinase. Upon activation by extracellular stimuli (nutrients, growth factors, mitogen, hormones, and stress), mTOR participates in the regulation of cell proliferation and metabolism (Dazert and Hall, 2011). The key molecules of mTOR signaling that regulate cell proliferation are p70 ribosomal S6 kinase (p70S6K) and eIF4E binding proteins (4E-BPs) (Klann and Dever, 2004).

Therefore, we hypothesized that the neuroprotective function of endogenous IL-6 from MSCs in HIBD rats might partially occur *via* the regulation of reactive astrocyte proliferation. A series of experiments were conducted to verify the above hypothesis. We first evaluated the biological role of IL-6 secreted by MSCs on astrocyte proliferation in neonatal HIBD rats. Next, a co-culture model of OGD-injured astrocytes and MSCs was established *in vitro* to validate the correlation between the therapeutic effects of MSCs on cell proliferation and endogenous IL-6. Finally, the potential mechanisms through which MSCs-derived IL-6 boosts the behavioral improvement in the HIBD model were revealed.

2. Methods

2.1. Animal groups

All animal experimental protocols were approved by the Animal Experimentation Ethics Committee of the Zoology Center at Chongqing Medical University (Chongqing, China). Sprague Dawley (SD) rats (8 weeks old) were purchased and housed in a specific pathogen-free (SPF) laboratory with a constant temperature of 22–24 °C, 60% relative humidity and artificial daylight from 07:00 to 19:00 every day at the Experimental Animal Center of Chongqing Medical University [SCXK (Yu) 2012-0015]. Food and water were provided *ad libitum*. After they were acclimated to the living environment for 3 days, the female rats were mated with the male rats in a 1:1 ratio and were checked for pregnancy.

When the pups were born and reached 7 days of age, they were used to establish the HIBD model as reported previously (Rice et al., 1981). Briefly, the left carotid artery was permanently ligated in 7-day-old postnatal rats. Two hours later, the pups were exposed to 8% oxygen at 37 °C for 2.5 h and then returned to their dams. All pups were randomly assigned to one of the following seven groups: sham, HIBD, HIBD + MSCs, HIBD + small interfering RNA (siRNA)-control MSCs, HIBD + siIL-6 MSCs, HIBD + vehicle and HIBD + rapamycin. The numbers of males and females in each group were approximately equal. After 5 days of HIBD (Ben et al., 2011), the rats in the HIBD + MSCs, HIBD + siRNA-control MSCs and HIBD + siIL-6 MSCs groups were intracerebroventricularly injected with 2×10^5 MSCs with or without different treatments suspended in 5 μl of phosphate-buffered saline (PBS) (HyClone, USA) (Bi et al., 2014). The rat siIL-6-transduced recombinant lentivirus was constructed by NeuronBiotech Co., Ltd. We originally designed 4 different shRNA sequences: GR425, GR426, GR427 and GR428, as described previously (He et al., 2014). A vector expressing green fluorescent protein (GFP) with the control sequence (TTCTCCGAACGTGTCACGT) served as a negative control (siRNA-control MSCs). The siIL-6 and control siRNA-transduced recombinant lentiviruses were constructed to infect the MSCs. The virus titer for infection was 3.47×10^8. The injection site was 1.2 mm posterior to bregma, 1.4 mm to the left of the lambdoid suture and at a needle depth of 3.6 mm. The infusion rate was 1 μl/min for 5 min. The needle was left in place for 2 min and then withdrawn slowly. The pups in the HIBD group were injected with the same volume of PBS as the pups in the control group. The sham group only subjected to a cervical skin incision that was subsequently sutured. For the rapamycin treatment, a stock solution of rapamycin was made in dimethyl sulfoxide (DMSO) (10 mg/ml) and diluted with vehicle solution (5% Tween 80 + 5% polyethylene glycol 400) to a final concentration of 0.1 mg/ml prior to use. Rapamycin was given intraperitoneally (6 mg/kg/day) once daily for 7 days (van Vliet et al., 2012).

2.2. Morris water maze test

When the rats in the sham group (n = 15), HIBD group (n = 15), HIBD + MSCs group (n = 15), HIBD + siRNA-control MSCs group (n = 15), HIBD + siIL-6 MSCs group (n = 15), HIBD + vehicle group (n = 15) and HIBD + rapamycin group (n = 15) reached four weeks of age, they were trained on the Morris water maze (MWM SLY-WMS 2.0, China) to evaluate their spatial learning and memory abilities as previously described (Morris, 1984). Briefly, the procedure lasted for six days. The first day consisted of the visible platform tests to assess their visual capabilities. On the next 4 days, the rats were trained to enhance their learning and memory function using the invisible platform. On the sixth day, a probe trial was performed without a platform.

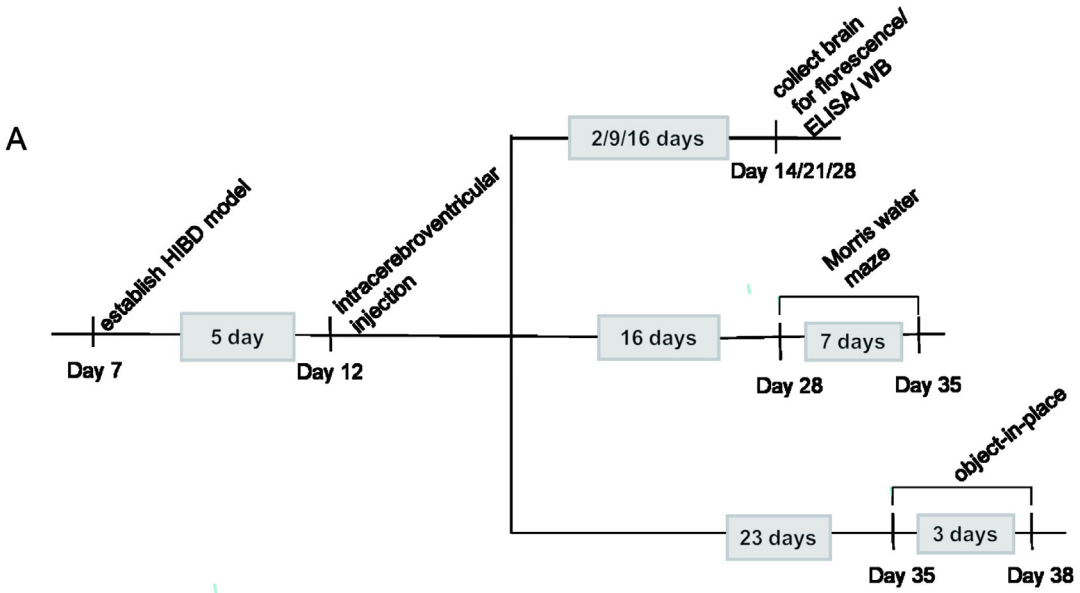

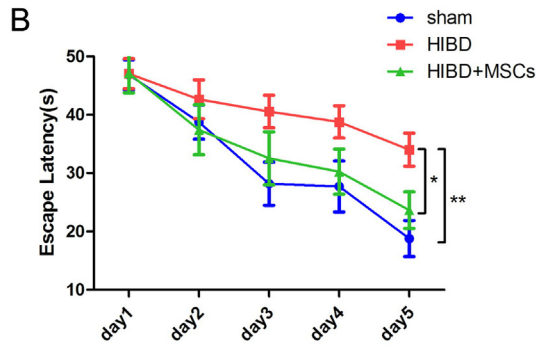

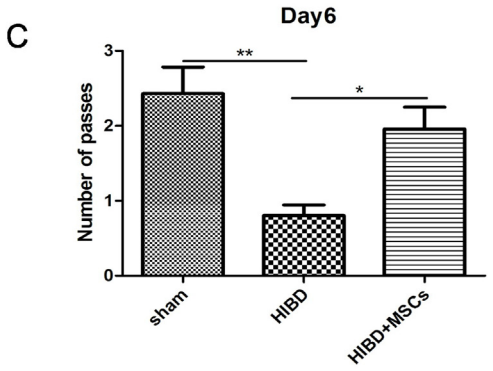

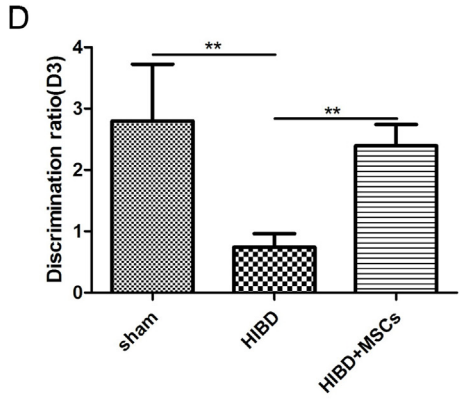

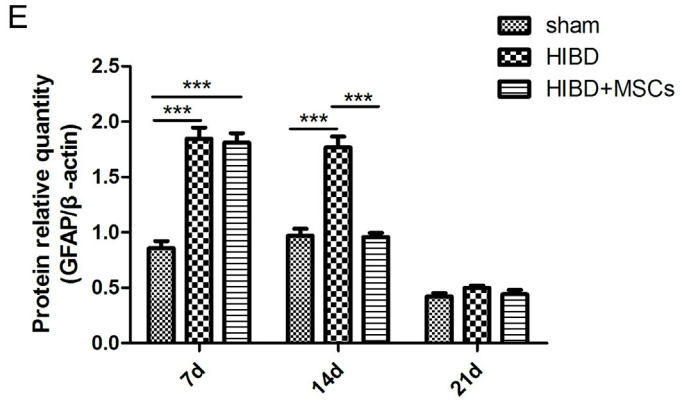

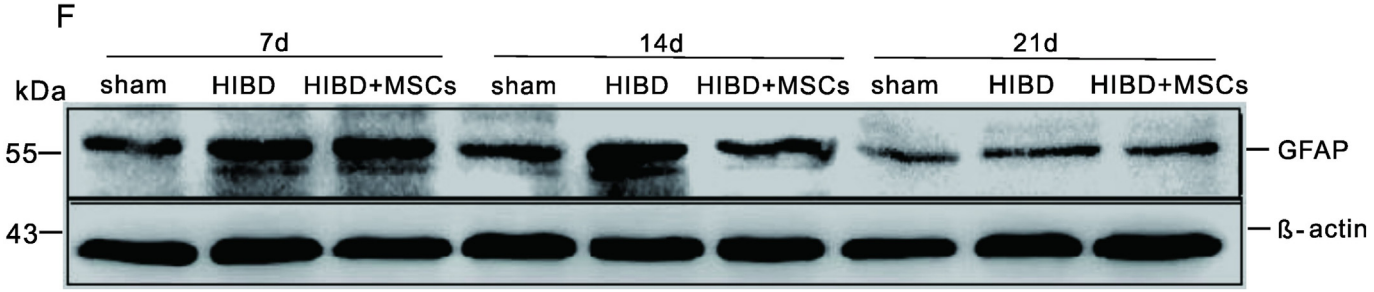

(caption on next page)

Fig. 1. MSCs transplantation restores the learning and memory function and decreases the expression level of GFAP in neonatal HIBD rats. (A) Diagram illustrating the experimental protocols of the treatments and tests for the rats in the different groups *in vivo*. (B) The escape latency of the sham, HIBD, and HIBD + MSCs groups on training days 1 to 5 in the Morris water maze test. (C) The number of passes through the platform region by the different treatment groups in the probe trial on day 6. (D) The discrimination ratio of the exploration time during the test phase of the object-in-place task for the three groups. (E-F) The protein expression level of GFAP in the hippocampal tissues collected from the three groups at 7, 14, and 21 days following HIBD and normalized to β-actin. Representative images are shown. The results are presented as the mean ± SEM. $^{*}P < 0.05$, $^{**}P < 0.01$, $^{***}P < 0.001$. n in the behavior test refers to the number of rats (n = 15). n in WB refers to the number of independent experiments (n = 3).

2.3. Object-in-place task

Five-week-old rats from the seven groups were subjected to an object-in-place task comprising a sample phase and a test phase as previously described (Zhou et al., 2015). During the test phase, the time spent exploring the four objects was recorded. The ratio of the time spent exploring between the two changed position objects and the other two unchanged position objects was expressed as the discrimination ratio (d3) (a relative measure of discrimination) (Barker and Warburton, 2011; Akkerman et al., 2012). An intact object-in-place memory is exhibited by rats spending more time investigating the two objects in different locations than the two objects in the same locations.

2.4. Preparation and treatment of primary astrocytes

Rat primary astrocytes were prepared from 2-day-old neonatal rats as described previously (Madrigal et al., 2006). Briefly, hippocampal tissue was stripped from the 2-day-old SD rats. Cells were mechanically dissociated in culture medium containing 10% fetal bovine serum (FBS) and then plated at 2×10^5 cells/cm^2 in a poly-L-lysine-precoated 10-cm dish. The hippocampal astrocytes were cultured for 5 days in an incubator containing 5% CO_2 (Thermo, USA). Immunofluorescence staining for goat anti-GFAP (Santa Cruz, sc-6170, USA) indicated that 95% of the cells were astrocytes. Then, these cells were cultured with EBSS medium and exposed to 5% O_2/5% CO_2 for 1.5 h to induce OGD injury as described previously (Madrigal et al., 2006). Astrocytes cultured in DMEM/F12 supplemented with 10% FBS in the presence of ambient (16%) O_2/5% CO_2 served as controls. The OGD-injured cells were then immediately administered different treatments. A subset of the OGD-injured cells was treated with separate co-cultures of MSCs, siIL-6 MSCs or siRNA-control MSCs in a Transwell insert (Gu et al., 2016). For the rapamycin treatment, these OGD-injured astrocytes were incubated in DMEM/F12 containing 10% FBS with 100 nM rapamycin according to our pre-experiment and others (Ji et al., 2013). The culture medium with or without rapamycin was replaced every 24 h. After 48 h, the culture medium and cells were collected from each group, and the total protein was extracted using a commercial kit (BioTek, China).

2.5. Immunofluorescence staining

The pups were sacrificed at 7 days, 14 days and 21 days after HIBD, and the brain tissues from the rats of each group were collected and fixed with 4% paraformaldehyde (Gu et al., 2016). After the brain tissues were dehydrated with 30% sucrose paraformaldehyde, 16-μm thick brain slices were sectioned using a Leica CM3050 S cryostat. For the immunofluorescence double staining, these brains sections were incubated in rabbit anti-Ki67 (Abcam, ab16667, USA) together with goat anti-GFAP (Santa Cruz, sc-6170, USA) overnight at 4 °C. Binding was visualized using Alexa Fluor 488-conjugated chicken anti-rabbit IgG (Life Technologies, USA) and Alexa Fluor 594-conjugated donkey anti-goat IgG (Jackson, USA), and the nuclei were stained with 4′,6-diamidino-2-phenylindole (DAPI, Yeasen). Four independent experiments were conducted.

For *in vitro* immunofluorescence staining (Gong et al., 2013), astrocytes were incubated with mouse anti-gp130 (Santa Cruz, sc-376,280, USA) or rabbit anti-AMPKα (Thr172) (Abcam, ab32047, USA) antibodies overnight at 4 °C. Binding was visualized using Alexa Fluor 488-conjugated chicken anti-mouse IgG (Life Technologies, USA) and Alexa Fluor 555-conjugated donkey anti-rabbit IgG (Life Technologies, USA), and the nuclei were stained with DAPI (Yeasen, Shanghai, China). Three independent experiments were conducted. The images were captured using an automatic biological fluorescence microscope (Nikon, Japan).

2.6. Enzyme-linked Immunosorbent Assay (ELISA)

IL-6 expression in the hippocampal tissues from the different treatment groups was detected using an ELISA from Beijing 4A Biotech Co., Ltd. (China). The levels of IL-6 released in the astrocyte culture medium were measured using an ELISA kit (RayBiotech, Inc., Norcross, GA, USA). The colorimetric optical density at 450 nm was recorded using a microtiter plate reader (Thermo). The cytokine levels were calculated based on a standard curve constructed for each assay. Three independent experiments were included in the analyses.

2.7. Protein preparation, Co-immunoprecipitation (Co-IP), and western blotting

Total protein extracted from the hippocampal tissues or primary astrocytes was used for western blotting. For the immunoprecipitation analysis (Hou et al., 2015), total protein extracted from the astrocytes was incubated with 2 μg of mouse anti-gp130 (Santa Cruz, sc-376,280, USA) or control IgG antibodies and protein-A agarose beads (Beyotime, China) overnight at 4 °C. Immunoprecipitates were washed and boiled, followed by western blotting. Samples of approximately 30 μg of protein were loaded into each lane of an 8% gel for sodium dodecyl sulfate-polyacrylamide gel electrophoresis (SDS-PAGE) (Beyotime, China) and transferred to 0.45 μm polyvinylidene fluoride membranes (Millipore, USA) after electrophoretic separation. All membranes were then blocked with 5% bovine serum albumin (BSA) (GenView, USA) at room temperature for 1 h and probed at 4 °C overnight with the following primary antibodies: rabbit anti-GFAP (Abcam, ab10062, USA), rabbit anti-AMPKα (Abcam, ab32047, USA), rabbit anti-gp130 (Abcam, ab202850, USA), rabbit anti-p-AMPKα (Thr172) (Cell Signaling, 2535 s, USA), rabbit anti-p-mTOR (Ser2448) (Cell Signaling, 5536 s, USA), rabbit anti-mTOR (Cell Signaling, 2972 s, USA), rabbit anti-p-p70S6K (Cell Signaling, 9205 s, USA) and rabbit anti-p-4E-BP1 (Cell Signaling, 2855 s, USA). HRP-conjugated secondary antibodies (Santa Cruz, USA) were applied at room temperature for 1 h and visualized using an enhanced chemiluminescence kit (Millipore, USA) with an ECL Imaging System (SynGene GBOX, UK). The results were quantified using ImageJ software. Three independent experiments were performed.

2.8. Ca^{2+} imaging in live cells

Primary astrocytes cultured in 24-well plates were subjected to OGD injury as described above. The cytoplasmic Ca^{2+} concentration ($[Ca^{2+}]c$) in the OGD-injured astrocytes was detected at 24 h after injury. Astrocytes were probed with 3 μM Fluo-4-AM (Dojindo, Japan) in 200 μl of HEPES-buffered Hank's Balanced Salt Solution (HBSS) at 37 °C for 30 min. Fluo-4-AM-labeled cells were observed using an inverted microscope (Nikon, Japan) with excitation and emission wavelengths of 488 nm and 520 nm, respectively. At least 100 cells from 3 random

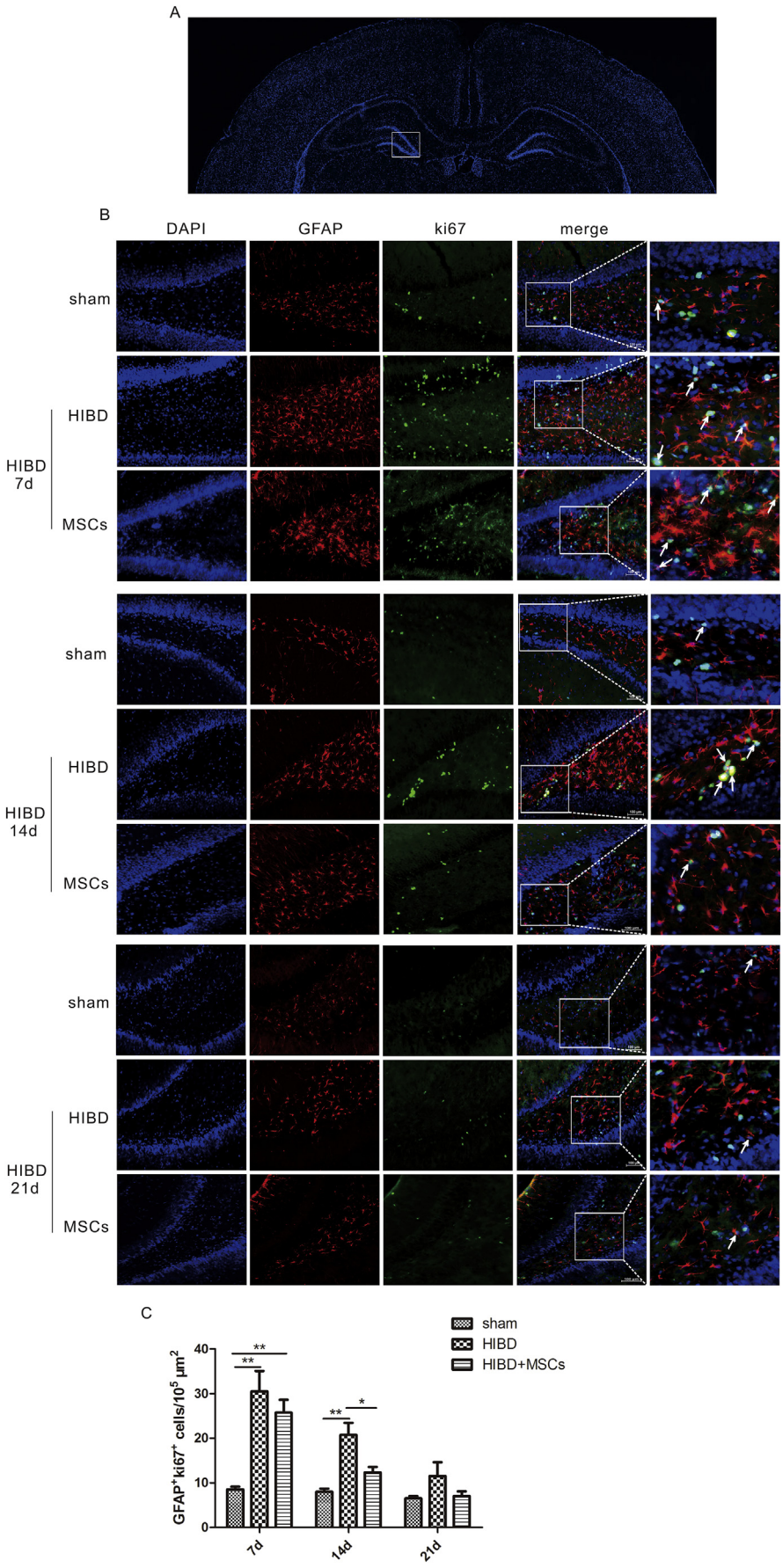

Fig. 2. MSCs transplantation suppresses astrocyte proliferation in the hippocampi of HIBD rats. (A) A coronal section of rat brain at 14 days after HIBD. The white box shows the dentate gyrus (DG) region of the hippocampus. (B) Double immunofluorescence staining for GFAP and Ki67 in the hippocampi of the sham, HIBD, and HIBD + MSCs groups at 7, 14, and 21 days following HIBD treatment. (C) Fluorescence quantification was performed according to the number of $GFAP^+/Ki67^+$ cells in the DG region of the hippocampus. The white arrows indicate the co-localization of GFAP and Ki67. Scale bar = 100 μm. The results are presented as the mean ± SEM. $^*P < 0.05$, $^{**}P < 0.01$. n = 4. n refers to the number of independent experiments.

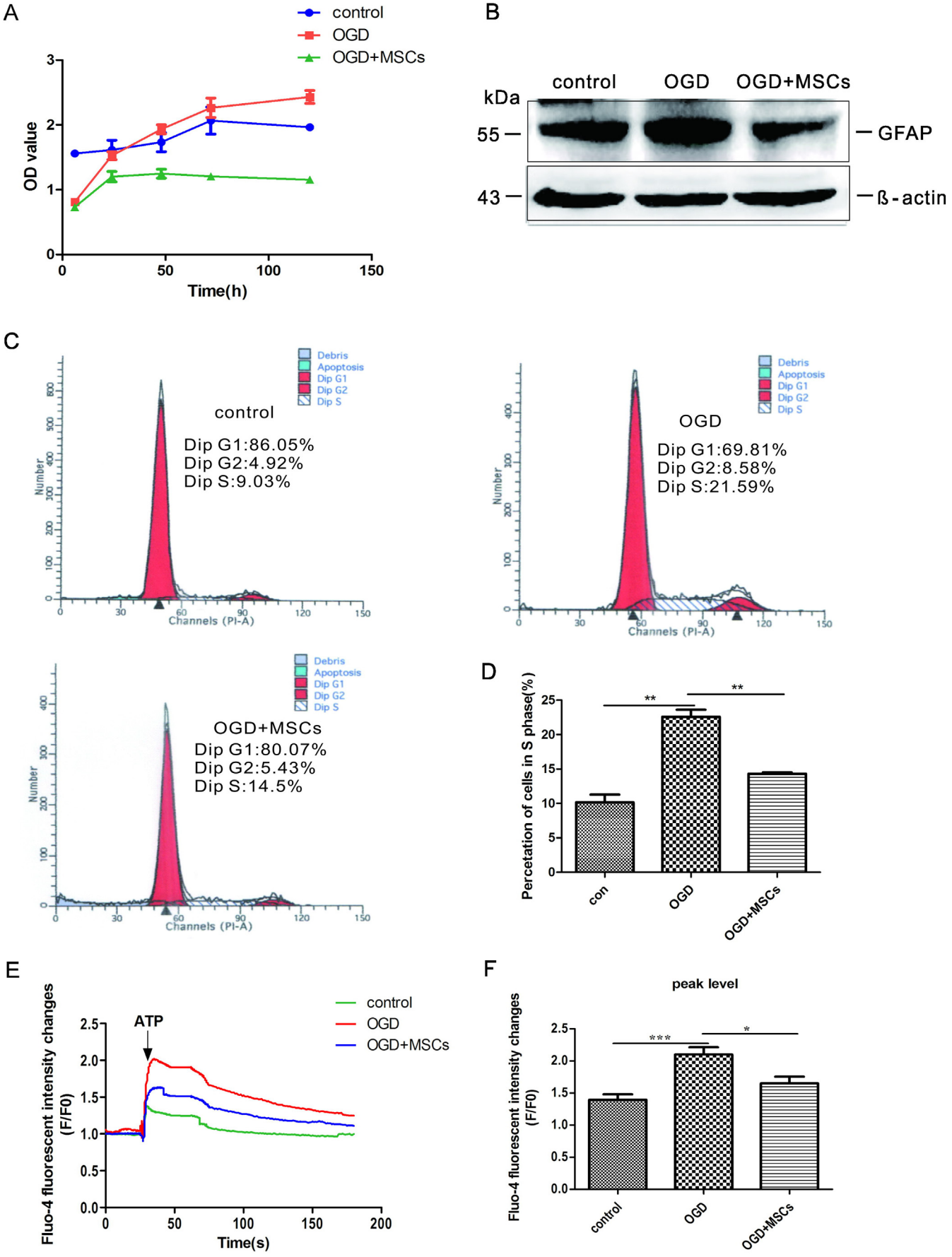

(caption on next page)

Fig. 3. MSCs co-culture attenuates the astrocyte proliferation induced by OGD injury *in vitro*. (A) Cell proliferation in the control, OGD, and OGD + MSCs groups was detected within 6–120 h by CCK-8. (B) Representative western blot images of GFAP expression in astrocytes in the three groups. (C) Representative images for flow cytometry analysis of the cell cycle progression of astrocytes in the three groups at 24 h. (D) The percentage of astrocytes in the S phase in the three groups. (E) Changes in the concentration of cytoplasmic Ca^{2+} ($[Ca^{2+}]_c$) in each group induced by ATP. (F) The peak values of the Fluo-4 fluorescence intensity in the three groups. The results are presented as the mean ± SEM. $^{*}P < 0.05$, $^{**}P < 0.01$, $^{***}P < 0.001$. n = 3. n refers to the number of independent experiments.

fields were counted in each group. The mean change in the fluorescence intensity (F) was normalized to the baseline fluorescence obtained prior to the addition of ATP to the wells (F_0). Three independent experiments were performed.

2.9. Cell proliferation and cell cycle analysis

For the cell proliferation analysis, rat astrocytes were seeded on a 24-well plate at a density of 3×10^4 viable cells per well and administered different treatments as described above. The culture medium was replaced every 24 h. Cell proliferation was detected at 6, 24, 48, 72, 96, and 120 h after OGD injury using Cell Counting Kit (CCK)-8. Here, 20 μl of CCK-8 solution was added to each well with 200 μl of culture medium and incubated for 3 h at 37 °C. The absorbance was measured at 450 nm using a microplate reader (Thermo, USA).

For the cell cycle analysis, 5×10^6 cells per well were inoculated on a 6-well plate. At 24 h after OGD injury, the astrocytes were digested with trypsin (without ethylenediaminetetraacetic acid (EDTA)), washed with ice-cold PBS (pH 7.4), fixed in ice-cold 70% ethanol, and stored at 4 °C. The cells were then washed with PBS, treated with 500 U/ml RNase (Sigma) at 37 °C for 15 min, and finally stained with propidium iodide (50 μg/ml, Sigma) in PBS. Cell cycle analysis was performed using a BD FACSCanto II flow cytometer (Becton Dickinson). For the detailed analysis, three cell cycle compartments (G1, S, and G2 phases) were divided, and the percentage of cells was quantified with CELLQuest software (Becton Dickinson). The experiments were repeated three times.

2.10. Statistical analysis

Statistical analyses were performed using GraphPad Prism 5.0 software. The values are expressed as the mean ± standard error of the mean (SEM). One-way analysis of variance (ANOVA) was used in the behavioral studies. For the biochemical studies, statistical analyses were performed using Student's *t*-tests. Significance was set at $P < 0.05$. In addition, a *post hoc* statistical power calculation was performed (Faul et al., 2007), which indicated that we had 100% power to detect a difference in the different treatment groups, with alpha set at 0.05.

3. Results

3.1. MSCs transplantation restored the learning-memory function and decreased the number of proliferating astrocytes in the hippocampi of HIBD rats

To elucidate the therapeutic function of MSCs transplantation in HIBD rats, learning and memory function tests were performed. As illustrated in Fig. 1B, on the 1st day of training in the Morris water maze, the escape latency and path length required to locate the platform did not significantly differ among the sham, HIBD, and HIBD + MSCs groups, indicating that neither HIBD nor MSCs transplantation impaired the motility and vision of the rats (Fig. 1B). The navigation test on days 2–5 revealed that the exploration time required to find the platform gradually shortened across training days in all three groups; however, the rats in the HIBD + MSCs group required less time to find the platform than those in the HIBD group ($^{*}P < 0.05$, *vs.* HIBD group), although the escape latency of the HIBD + MSCs group was slightly longer than that of the sham group. In the platform exploration test on day 6, the rats that received MSCs transplantation entered the platform region significantly more than the HIBD rats ($^{*}P < 0.05$, *vs.* HIBD group, Fig. 1C). The object-in-place task results demonstrated that the total exploration time was similar among the three groups (data not shown), indicating no deficits in locomotor activity. The exploration behavior analysis demonstrated that HIBD rats spent significantly less time exploring the toys whose position had been changed than the rats in the HIBD + MSCs and sham groups ($^{**}P < 0.01$, *vs.* HIBD group), while there was no significant difference between the HIBD + MSCs and sham groups (Fig. 1D). The above results indicated that MSCs transplantation enhanced the memory ability of HIBD rats, which was consistent with the results of previous studies (Gu et al., 2016). In addition, our study showed that MSCs treatment significantly reduced the protein expression of GFAP at 14 days after HIBD in the hippocampi compared to HIBD treatment alone ($^{***}P < 0.001$, *vs.* HIBD group Fig. 1E-F). Double immunostaining further revealed that 7 days after HIBD, significantly more $GFAP^+/Ki67^+$ double-labeled cells were found in the hippocampi of the HIBD and HIBD + MSCs rats than in those of the sham rats ($^{**}P_{HIBD} < 0.01$, $^{**}P_{MSCs} < 0.01$, *vs.* sham group). However, MSCs transplantation significantly reduced the number of $GFAP^+/Ki67^+$ double-labeled cells in the hippocampi of the HIBD rats on day 14 after HIBD ($^{*}P < 0.05$, *vs.* HIBD group, Fig. 2B-C). At 21 days after HIBD, the number of $GFAP^+/Ki67^+$ cells had returned to sham level in both HIBD and HIBD + MSCs groups. These results suggested that MSC transplantation could significantly suppress the proliferation of hippocampal astrocytes in HIBD rats.

3.2. MSCs co-culture in vitro suppressed the proliferation of astrocytes induced by OGD injury

To further validate the effect of MSCs on the proliferation of injured astrocytes, an *in vitro* co-culture model of MSCs and rat primary astrocytes injured by OGD was used to detect the proliferation of injured cells at different time points. As shown in Fig. 3A, the cells in the OGD and OGD + MSCs groups displayed obvious proliferation within 24 h of injury. After 48–120 h of OGD, the cells in the OGD group continued to exhibit persistent and rapid proliferation; in contrast, the astrocyte proliferation rate was reduced when co-cultured with MSCs. In addition, OGD injury increased GFAP protein expression, which was effectively suppressed by MSCs co-culture (Fig. 3B). Further evaluation of the changes in the cell cycle of astrocytes after OGD injury by flow cytometry revealed that the percentage of S phase cells in the OGD + MSCs group was significantly decreased compared with that in the OGD group ($^{**}P < 0.01$, *vs.* OGD group, Fig. 3C–D). As illustrated in Fig. 3E–F, evaluation of the intracellular changes in Ca^{2+} using a calcium imaging system revealed that ATP induced a significantly transient increase in the cytoplasmic Ca^{2+} level in OGD-injured astrocytes, while MSCs co-culture significantly suppressed the release of intracellular Ca^{2+} induced by ATP ($^{*}P < 0.05$, *vs.* OGD group). The above results indicated that MSCs co-culture could reduce the proliferation of astrocytes induced by OGD injury and decrease intracellular Ca^{2+} release.

3.3. MSCs promoted the expression of gp130 and p-AMPKα but downregulated mTOR signaling in OGD-injured astrocytes

Our previous work has demonstrated that the neuroprotective function of MSCs is closely associated with their secretion of IL-6 (Gu

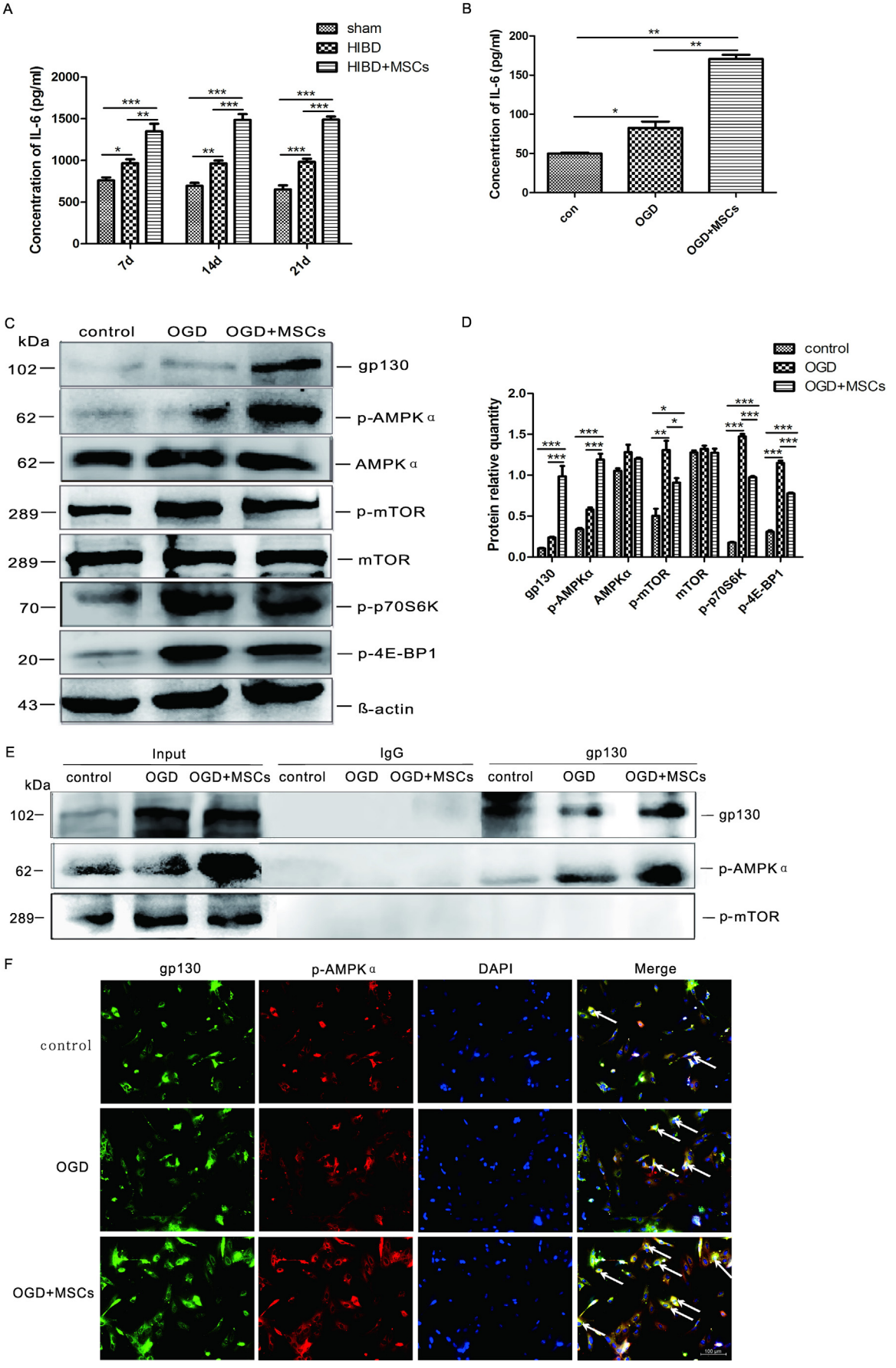

(caption on next page)

Fig. 4. MSCs facilitate the expression levels of gp130 and p-AMPKα but downregulate mTOR signaling in OGD-injured astrocytes. (A) The concentration of IL-6 in the hippocampi of rats in the sham, HIBD and HIBD + MSCs groups at 7, 14 and 21 days after HIBD treatment. (B) The level of IL-6 protein released in the culture medium of the control, OGD and OGD + MSCs groups *in vitro* as determined by ELISA. (C–D) The protein expression levels of gp130, p-AMPKα, p-mTOR, p-p7S6K and p-4E-BP1 in the astrocytes of the three groups and normalized to β-actin. (E) Co-IP was performed to determine the interaction between gp130 and p-AMPKα or p-mTOR in the astrocytes among the control, OGD and OGD + MSCs groups. (F) The subcellular distribution of gp130 and p-AMPKα in the three groups as determined using immunofluorescence staining. The white arrows indicate the co-localization of gp130 and p-AMPKα. Scale bar = 100 μm. Representative images are shown. The results are presented as the mean ± SEM. $^{*}P < 0.05$, $^{**}P < 0.01$, $^{***}P < 0.001$. n = 3. n refers to the number of independent experiments.

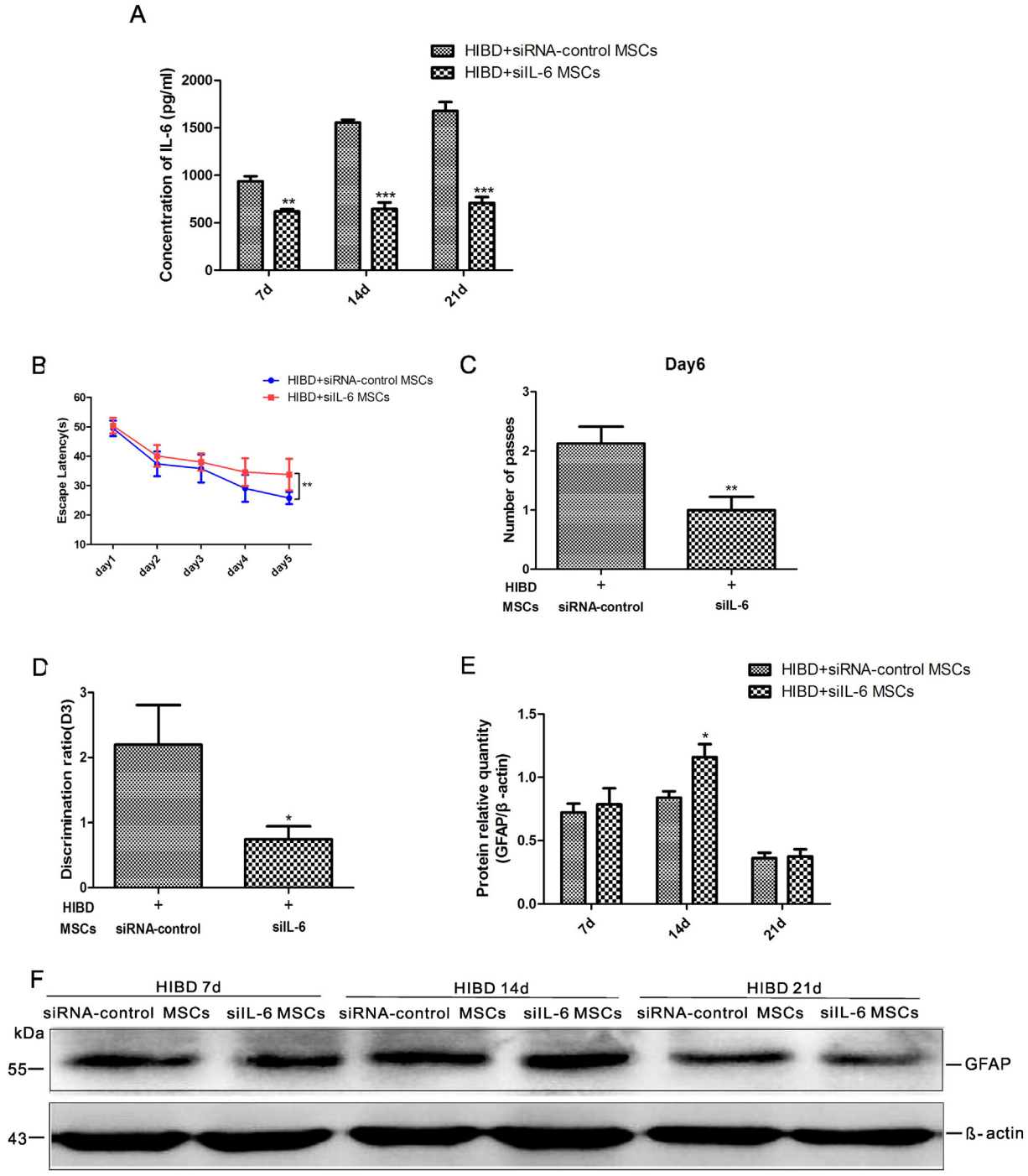

Fig. 5. siIL-6 MSCs transplantation impairs the learning and memory function and increases the level of GFAP expression in neonatal HIBD rats. (A) The concentration of IL-6 protein in the hippocampal tissues at 7, 14, and 21 days following MSCs transplanted by siRNA-control MSCs or HIBD + siIL-6 MSCs. (B) The escape latency of the two groups on the hidden platform tests from day 1–5 in the Morris water maze test. (C) Number of platform region entries of the two groups during the probe trial on day 6. (D) Discrimination between the novel (changed position) and familiar objects (unchanged position) in the two groups. (E-F) The GFAP protein expression levels in the hippocampal tissues from the two groups at 7, 14, and 21 days after HIBD and normalized to β-actin. Representative image are shown. The results are presented as the mean ± SEM. $^{*}P < 0.05$, $^{**}P < 0.01$, $^{***}P < 0.001$. n in behavior test refers to the number of rats (n = 15). n in WB or ELISA refers to the number of independent experiments (n = 3).

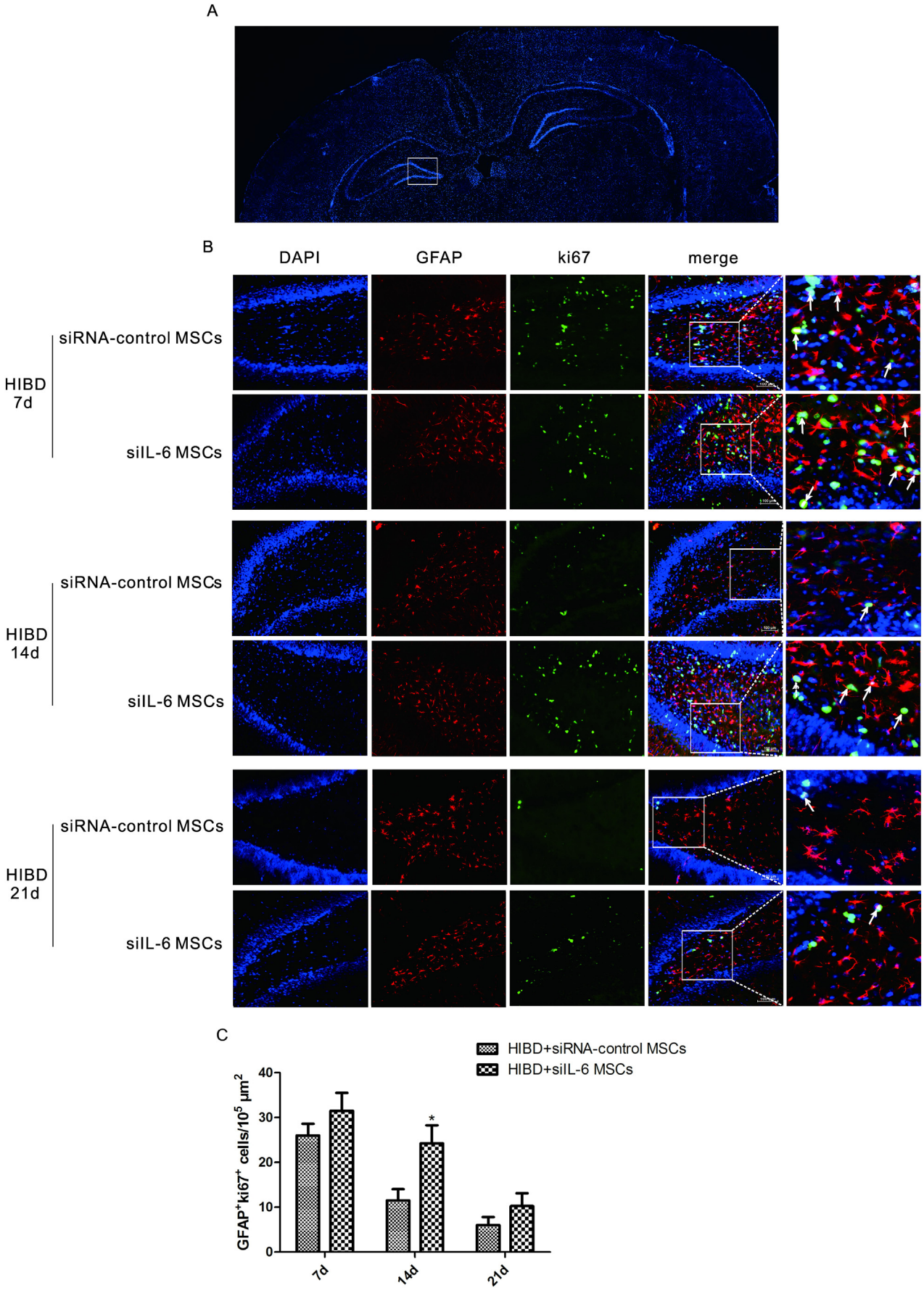

(caption on next page)

Fig. 6. siIL-6 MSCs transplantation enhances astrocytes proliferation in the hippocampi of HIBD rats. (A) Coronal section of rat brain at 14 days after HIBD and immunostained for DAPI. The white box shows the DG region of the hippocampus. (B) The number of astrocytes double-stained for GFAP and Ki67 in the hippocampi of HIBD rats at 7, 14, and 21 days following siRNA-control MSCs or siIL-6 MSCs transplantation. The white arrows indicate the co-localization of GFAP and Ki67. (C) Quantification of the number of $GFAP^+/Ki67^+$ cells in the DG region of the hippocampus. Scale bar = 100 μm. The results are presented as the mean ± SEM. $^*P < 0.05$. n = 4. n refers to the number of independent experiments.

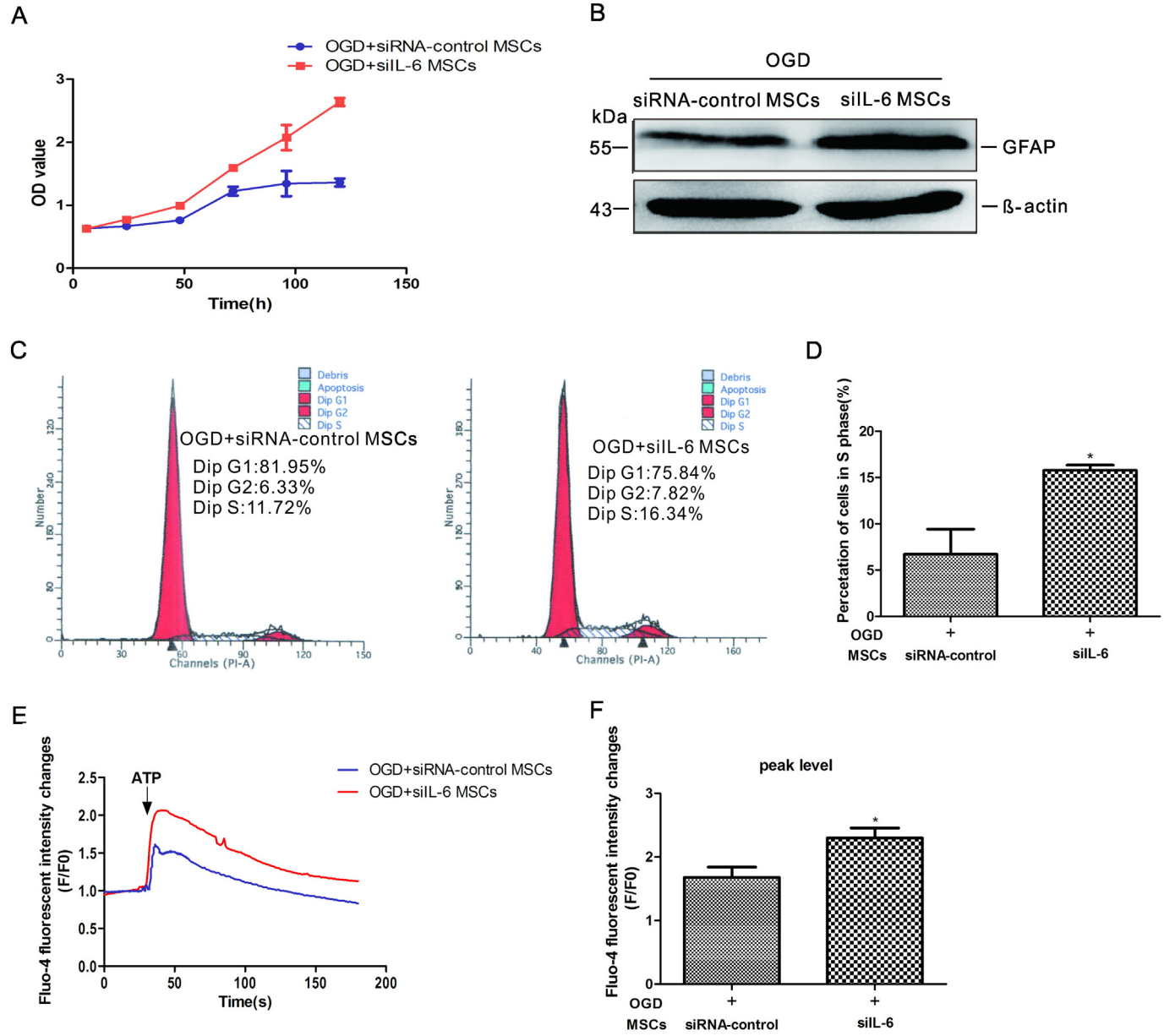

Fig. 7. siIL-6 MSCs accelerate the proliferation of astrocytes injured by OGD. (A) Changes in cell proliferation in the OGD astrocytes following co-culture with siRNA-control MSCs or siIL-6 MSCs, as detected within 6–120 h by CCK-8. (B) Representative western blot images of the GFAP expression levels in the astrocytes between the OGD + siRNA-control MSCs and OGD + siIL-6 MSCs groups. (C) Representative images of the flow cytometry analysis of the OGD-injured astrocytes' cell cycle in the two treatment groups at 24 h. (D) The percentage of the astrocytes in the S phase between the OGD + siRNA-control MSCs and OGD + siIL-6 MSCs groups. (E) Changes in the cytoplasmic Ca^{2+} ($[Ca^{2+}]_c$) levels of the two groups induced by ATP. (F) The peak values of the Fluo-4 fluorescence intensity of the two groups. The results are presented as the mean ± SEM. $^*P < 0.05$. n = 3. n refers to the number of independent experiments.

et al., 2016). Therefore, we focused on the AMPK/mTOR signaling pathway, which is supposed to be a downstream pathway of IL-6 and involved in cell proliferation (Ruderman et al., 2006; White et al., 2013; Jia et al., 2016). Hippocampal tissues of HIBD rats and astrocyte culture medium were first collected and analyzed by ELISA. MSCs treatment significantly increased IL-6 secretion levels in the hippocampi of rats after 7, 14, and 21 days of HIBD ($^{**}P_{7d} < 0.01$, $^{***}P_{14d} < 0.001$, $^{***}P_{21d} < 0.001$, *vs.* HIBD group, Fig. 4A) and in the co-culture system *in vitro* ($^{**}P < 0.01$, *vs.* OGD group, Fig. 4B). MSCs co-culture *in vitro* also promoted the protein expression of gp130 and p-AMPKα in the OGD-injured astrocytes, and reduced the expression levels of p-mTOR, p-p7S6K, and p-4E-BP1 compared to OGD treatment alone ($^{***}P_{gp130} < 0.001$, $^{***}P_{p\text{-}AMPK} < 0.001$, $^{*}P_{p\text{-}mTOR} < 0.05$, $^{***}P_{p\text{-}p7S6K} < 0.001$, $^{***}P_{p\text{-}4E\text{-}BP1} < 0.001$, *vs.* OGD group, Fig. 4C–D). The results of the Co-IP and immunofluorescence staining further revealed that gp130 interacted with p-AMPKα, but not p-mTOR, in the astrocytes

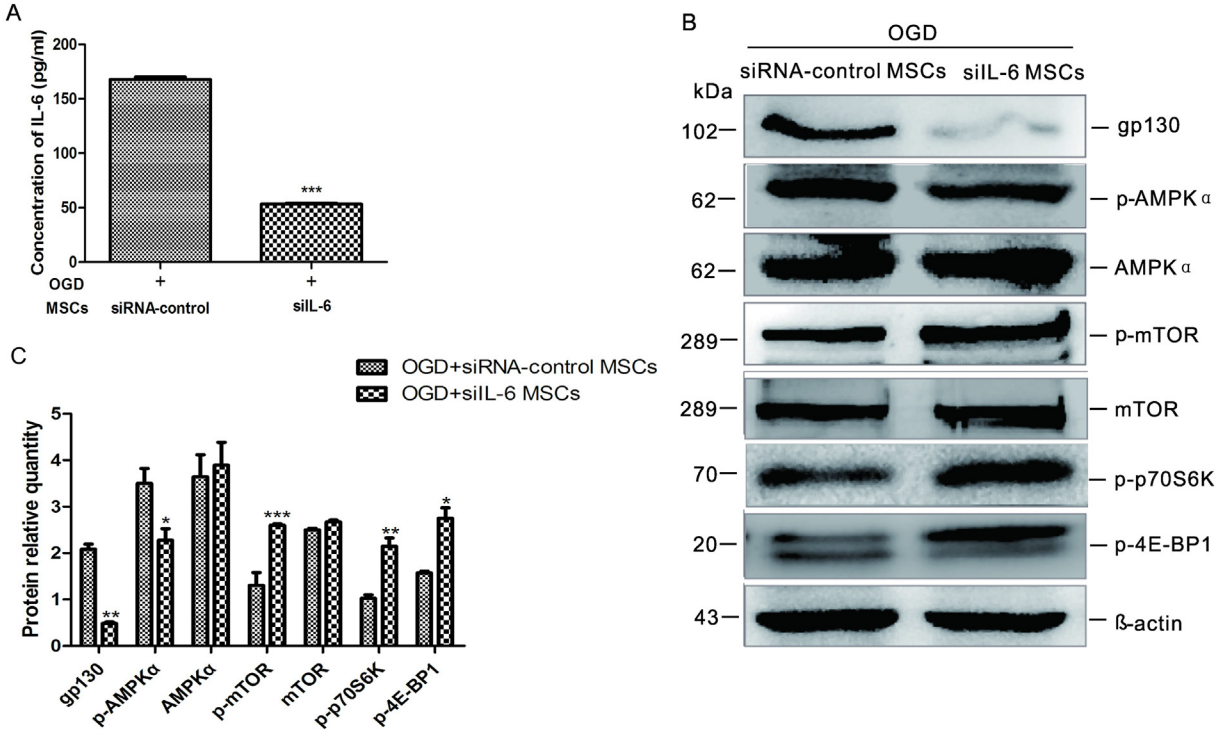

Fig. 8. siIL-6 MSCs suppress the expression levels of gp130 and p-AMPKα but induce mTOR signaling in OGD-injured astrocytes. (A) Changes in the IL-6 concentration in the culture medium of OGD-injured astrocytes following co-culture with either siRNA-control MSCs or siIL-6 MSCs. (B—C) Representative western blot images for gp130, p-AMPKα, AMPKα, p-mTOR, mTOR, p-p7S6K and p-4E-BP1 expression in the astrocytes of the OGD + siRNA-control MSCs and OGD + siIL-6 MSCs groups. The results were normalized to β-actin. Representative images are shown. The results are presented as the mean ± SEM. $^{*}P < 0.05$, $^{**}P < 0.01$, $^{***}P < 0.001$. n = 3. n refers to the number of independent experiments.

(Fig. 4E-F). Compared with OGD treatment alone, MSCs co-culture facilitated the interaction between p-AMPKα and gp130. The above results suggested that MSCs may modulate the proliferation of injured astrocytes by secreting IL-6 and activating the AMPK/mTOR signaling pathway.

3.4. siIL-6 MSCs transplantation impaired the learning and memory function and increased the number of proliferating astrocytes in the hippocampi of HIBD rats

To confirm the effect of endogenous IL-6 from MSCs on the proliferation of astrocytes after injury, HIBD rats were further treated with siIL-6 MSCs transplantation. As shown in Fig. 5A, compared to the rats in the HIBD + siRNA-control MSCs group, siIL-6 MSCs-transplanted rats expressed significantly lower IL-6 levels in the hippocampi at 7, 14, and 21 days ($^{**}P_{7d} < 0.01$, $^{***}P_{14d} < 0.001$, $^{***}P_{21d} < 0.001$). The Morris water maze test revealed that the escape latency to find the platform of the HIBD + siIL-6 MSCs rats was statistically longer than that of the HIBD + siRNA-control MSCs rats ($^{**}P < 0.01$, Fig. 5B). In addition, as shown in our previous study (Gu et al., 2016), the number of passes through the platform region in the spatial probe test was also significantly less in the HIBD + siIL-6 MSCs group than in the HIBD + siRNA-control MSCs group ($^{**}P < 0.01$, Fig. 5C). Similarly, in the object-in-place test, a comparison of the total object exploration time revealed no differences between the two groups (data not shown), indicating intact locomotor activity. The exploration behavior analysis for the object-in-place test demonstrated that the discrimination score of the rats in the HIBD + siIL-6 MSCs group was significantly decreased compared to that in the HIBD rats treated with the siRNA-control MSCs ($^{*}P < 0.05$, Fig. 5D). We also found that on day 14 after HIBD, the protein expression of GFAP ($^{*}P < 0.05$, Fig. 5E and F) and the number of $GFAP^{+}/Ki67^{+}$ double-labeled cells ($^{*}P < 0.05$, Fig. 6B and C) in the hippocampi of HIBD rats transplanted with siIL-6 MSCs were significantly greater than those in the hippocampi of HIBD rats transplanted with siRNA-control MSCs. OGD-injured astrocytes co-cultured with siIL-6 MSCs exhibited durative proliferation within 6–120 h following OGD, whereas cells in the OGD + siRNA-control MSCs group consistently displayed slow proliferation (Fig. 7A). In addition, the siIL-6 MSCs co-culture obviously elevated GFAP protein expression in the OGD-injured astrocytes (Fig. 7B). The percentage of S phase cells in the OGD + siIL-6 MSCs group was significantly higher than that in the OGD + siRNA-control MSCs group ($^{*}P < 0.05$, Fig. 7C and D). Furthermore, the OGD-injured astrocytes co-cultured with siIL-6 MSCs had intriguingly higher intracellular Ca^{2+} concentrations induced by ATP than those co-cultured with siRNA-control MSCs ($^{*}P < 0.05$, Fig. 7E and F). These data supported our hypothesis that MSCs-derived IL-6 plays a pivotal role in the proliferation of astrocytes after injury.

3.5. siIL-6 MSCs suppressed the expression levels of gp130 and p-AMPKα and activated mTOR signaling in the OGD-injured astrocytes

To further verify the speculation that MSCs-derived IL-6 plays a role in regulating astrocyte proliferation by activating the AMPK/mTOR signaling pathway, the current study established a co-culture model of siIL-6 MSCs and OGD-injured astrocytes. Our study *in vitro* demonstrated that with the significant reduction of IL-6 secretion in the siIL-6 MSCs co-culture system ($^{***}P < 0.001$, Fig. 8A), the protein expression of gp130 and p-AMPKα in the OGD-injured astrocytes also decreased accordingly, while the protein expression levels of p-mTOR, p-p7S6K, and p-4E-BP1 increased ($^{**}P_{gp130} < 0.01$, $^{*}P_{p\text{-}AMPK} < 0.05$, $^{***}P_{p\text{-}mTOR} < 0.001$, $^{**}P_{p\text{-}p7S6K} < 0.01$, $^{*}P_{p\text{-}4E\text{-}BP1} < 0.05$, Fig. 8B-C). These results further demonstrated that the IL-6 secreted by MSCs is a key factor in the modulation of injured astrocyte proliferation *via* activation of the AMPK/mTOR signaling pathway.

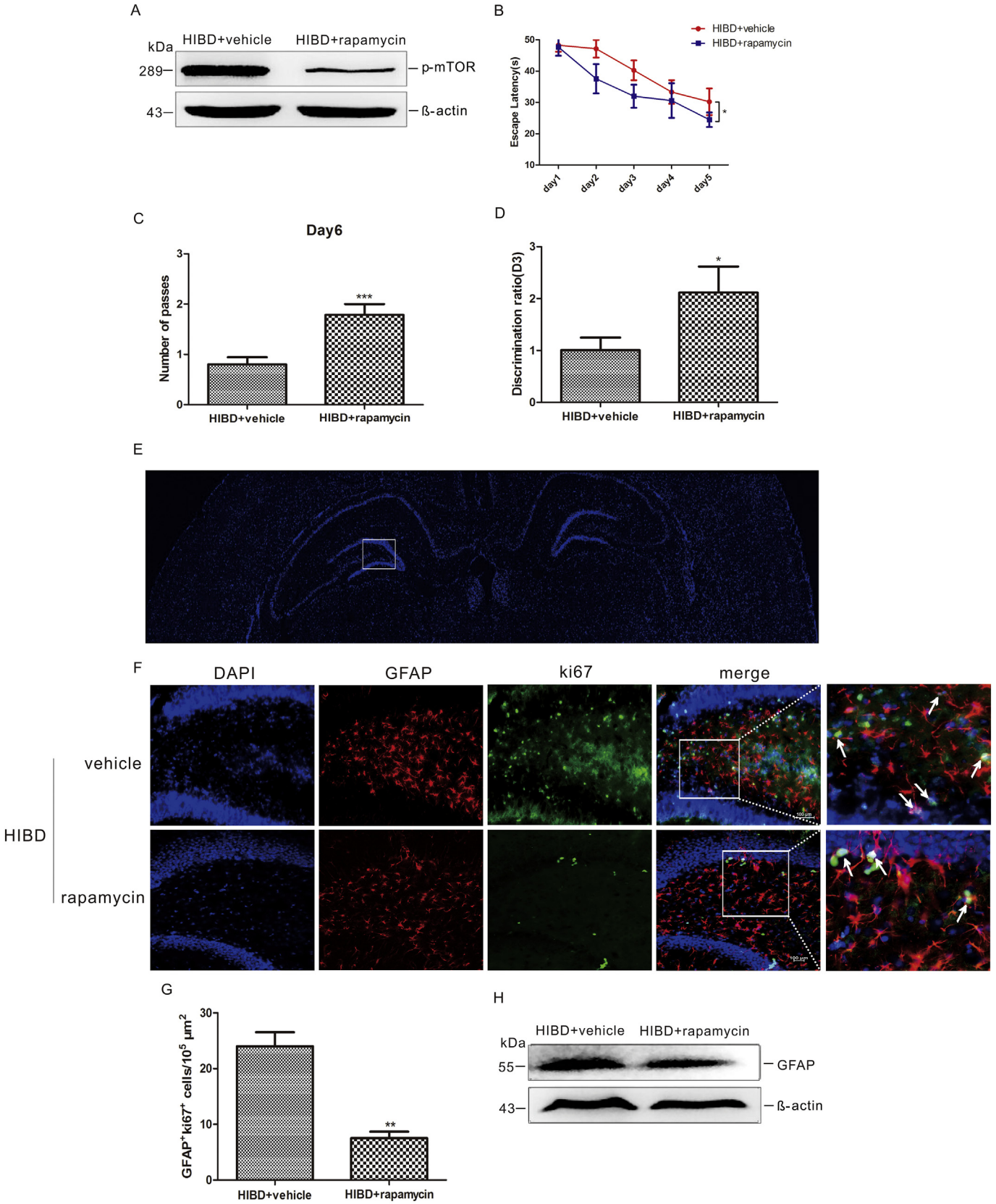

(caption on next page)

Fig. 9. Rapamycin suppresses astrocyte proliferation in the hippocampi to improve the learning and memory function of HIBD rats *via* reducing mTOR signaling. (A) Levels of p-mTOR protein expression in the hippocampal tissues of the HIBD + vehicle and HIBD + rapamycin groups were measured by western blotting. (B) The escape latency to locate the visible platform of the HIBD rats with or without rapamycin treatment from the 1st to 5th day in the Morris water maze test. (C) The number of times the rats in each group passed through the platform region during the probe trial on day 6 of the Morris water maze test. (D) The discrimination ratio of the exploration time during the test phase for the object-in-place task. (E) Brain coronal section showing DAPI staining at 14 days after HIBD. The white box shows the DG region of the hippocampus. (F) Co-localization of GFAP and Ki67 in the hippocampi of the HIBD rats after rapamycin treatment for 7 days. The white arrows indicate the co-localization of GFAP and Ki67. (G) Quantification analysis of the number of $GFAP^+/Ki67^+$ cells in the DG region of the hippocampus between the HIBD + vehicle and HIBD + rapamycin groups. (H) Representative western blot images for GFAP expression in the hippocampal tissues at day 7 after rapamycin treatment. Scale bar = 100 μm. The results are presented as the mean ± SEM. $^*P < 0.05$, $^{**}P < 0.01$, $^{***}P < 0.001$. n in behavior test refers to the number of rats (n = 15). n in WB refers to the number of independent experiments (n = 3).

3.6. Suppression of mTOR signaling reduced the proliferation of injured astrocytes to ameliorate the learning and memory function of HIBD rats

To further verify the regulatory role of mTOR in astrocyte proliferation to improve the learning and memory impairment of HIBD rats, we intraperitoneally injected HIBD rats with the mTOR-specific inhibitor rapamycin for 7 continuous days. As shown in Fig. 9A, rapamycin effectively suppressed the expression levels of p-mTOR in the hippocampal tissues of HIBD rats. The results of the Morris water maze test revealed that the exploration time required to find the platform by the rats in the HIBD + rapamycin group was significantly shorter than that in the HIBD + vehicle control group ($^*P < 0.05$, Fig. 9B). Additionally, the number of times the rats passed through the platform region on day 6 was also statistically increased in the HIBD + rapamycin group ($^{***}P < 0.001$, Fig. 9C). The total exploration time in the object-in-place test was similar between the HIBD + vehicle and HIBD + rapamycin groups (data not shown). During the test phase, the learning and memory ability of the rats in the HIBD + rapamycin group was significantly enhanced compared with that of the HIBD + vehicle group ($^*P < 0.05$, Fig. 9D). Additionally, 7 days of rapamycin intervention significantly decreased the number of $GFAP^+/Ki67^+$ double-labeled cells and GFAP protein expression in the hippocampi of HIBD rats ($^{**}P < 0.01$, Fig. 9E–H). OGD-injured astrocytes were also treated with rapamycin, which dramatically attenuated the proliferation rate of the injured cells, reduced GFAP protein expression (Fig. 10A and B), decreased the number of S phase cells ($^{**}P < 0.01$, Fig. 10C and D), and suppressed the intracellular Ca^{2+} concentration induced by ATP in the injured astrocytes ($^{***}P < 0.001$, Fig. 10E and F). Furthermore, rapamycin effectively inhibited expression of the p-mTOR, p-p7S6K, and p-4E-BP1 proteins in the OGD-injured astrocytes but had no effect on the expression of gp130 or p-AMPKα ($^{***}P_{p\text{-}mTOR} < 0.001$, $^{**}P_{p\text{-}p7S6K} < 0.01$, $_{***}P_{p\text{-}4E\text{-}BP1} < 0.001$, Fig. 10G and H). These results provided strong evidence supporting the previous conclusions that mTOR is involved in the regulation of astrocyte proliferation.

4. Discussion

The present study aimed to resolve whether IL-6 is a critical factor in the regulation of reactive astrocyte proliferation in HIBD rats following MSCs transplantation and its specific molecular mechanisms. Our data demonstrated that MSCs act on astrocytes to suppress cell proliferation *via* the production of IL-6 and the activation of its downstream AMPK/mTOR signaling pathway, thereby improving the learning and memory impairment of HIBD rats.

HIBD can lead to severe neurological disorders in children, such as mental retardation, cerebral palsy, and epilepsy (Low, 2004; Vannucci and Hagberg, 2004; Aridas et al., 2014). At the acute stage of cerebral ischemic injury, astrocytes protect neurons from oxidative stress (Li et al., 2008); however, if the excessive reactive proliferation at the early stage of chronic injury cannot be resolved, recovery of CNS function will be suppressed (Wanner et al., 2008; Sukumari-Ramesh et al., 2012). Therefore, investigating the switch in the role of reactive astrocytes and the dynamic course during HIBD is particularly important. One week after ischemic injury is usually regarded as the subacute stage. During this period, astrocytes undergo a response termed "astrogliosis", which is characterized by increased expression of GFAP, cell hypertrophy and proliferation (Anderson et al., 2003). Our study suggested that astrocytes exhibit marked proliferation at 7–14 days after HIBD *in vivo,* reached the peak at 14d and within 24 h of OGD injury *in vitro*, as well as a significant increase in GFAP expression. We also found that the number of $GFAP^+/Ki67^+$ cells returned to sham levels at 21 days after HIBD. The proliferation rules of astrocytes after HIBD is basically consistent with previous studies (Zhu et al., 2007b; Li et al., 2011), which suggests that appropriate time window must be mastered for the intervention of HIBD. OGD injury for 6–24 h *in vitro* is comparable to the subacute stage of ischemic injury *in vivo* (Wang et al., 2012). GFAP upregulation is an important step in astrocyte activation in response to various nervous system diseases (Choudhury and Ding, 2016). Therefore, GFAP is considered to be an effective marker of reactive astrocytes. Affymetrix GeneChip arrays used to profile gene expression in astrocytes at 7 days after middle cerebral artery occlusion (MCAO) demonstrated that reactive astrocytes at this stage may be beneficial or neuroprotective *via* the expression of high levels of many neurotrophic factors and cytokines (such as cardiotrophin-like cytokine factor 1 (CLCF1), leukemia inhibitory factor (LIF), IL-6, and thrombospondin) (Sofroniew, 2009; Zamanian et al., 2012).

MSCs provide potent therapeutic benefits for functional recovery following brain damage (van Velthoven et al., 2010b,c; Gu et al., 2016). In the current study, we also found that MSC transplantation ameliorated the learning and memory function of HIBD rats. The obvious astrocyte proliferation in the dentate gyrus (DG) region of the hippocampi was significantly decreased following MSCs transplantation for 2 weeks. Furthermore, MSCs co-cultured with astrocytes *in vitro* decreased both the proliferation rate of the astrocytes and the percentage of cells in S phase. Accumulative data have implied that MSCs may have protective effects on astrocytes (Gao et al., 2005a,b; Li et al., 2005), especially through the downregulation of reactive astrogliosis and reduction in the thickness of the scar wall (Li et al., 2005). Gao et al. also demonstrated that bone marrow stromal cells (BMSCs) may exert therapeutic benefits on animal models of ischemic stroke by maintaining the morphological integrity and proliferation of astrocytes (Gao et al., 2008). The astrocytic response in all CNS pathologies involves various molecular and morphological changes and may result in both a loss of normal function and a gain of abnormal effects. In mild-to-moderate injury, a timely therapeutic intervention may reverse these detrimental changes (Sofroniew, 2009). Treatment of HIBD with MSCs transplantation has been demonstrated to significantly downregulate the number of $GFAP^+$ cells and attenuate reactive astrogliosis 18 days later (Donega et al., 2014), which is largely consistent with the results of our study and indicates that MSCs exert their function at the chronic early stage of HIBD. Furthermore, our study showed that ATP induced an increase in intracellular Ca^{2+} in the OGD-injured astrocytes, which was suppressed by MSCs co-culture. A growing body of evidence has indicated that Ca^{2+} signaling participates in the regulation of cell proliferation, differentiation and apoptosis (Berridge et al., 2000). Increased intracellular Ca^{2+} has been reported to promote astrocyte proliferation (Florio et al., 1996), and application of rapamycin (an mTOR-specific inhibitor) represses the release of intracellular Ca^{2+} and the reflux of extracellular Ca^{2+} (Rice et al., 1981; Ogawa et al., 2009). Intriguingly, our results also suggested that rapamycin downregulated the ATP-

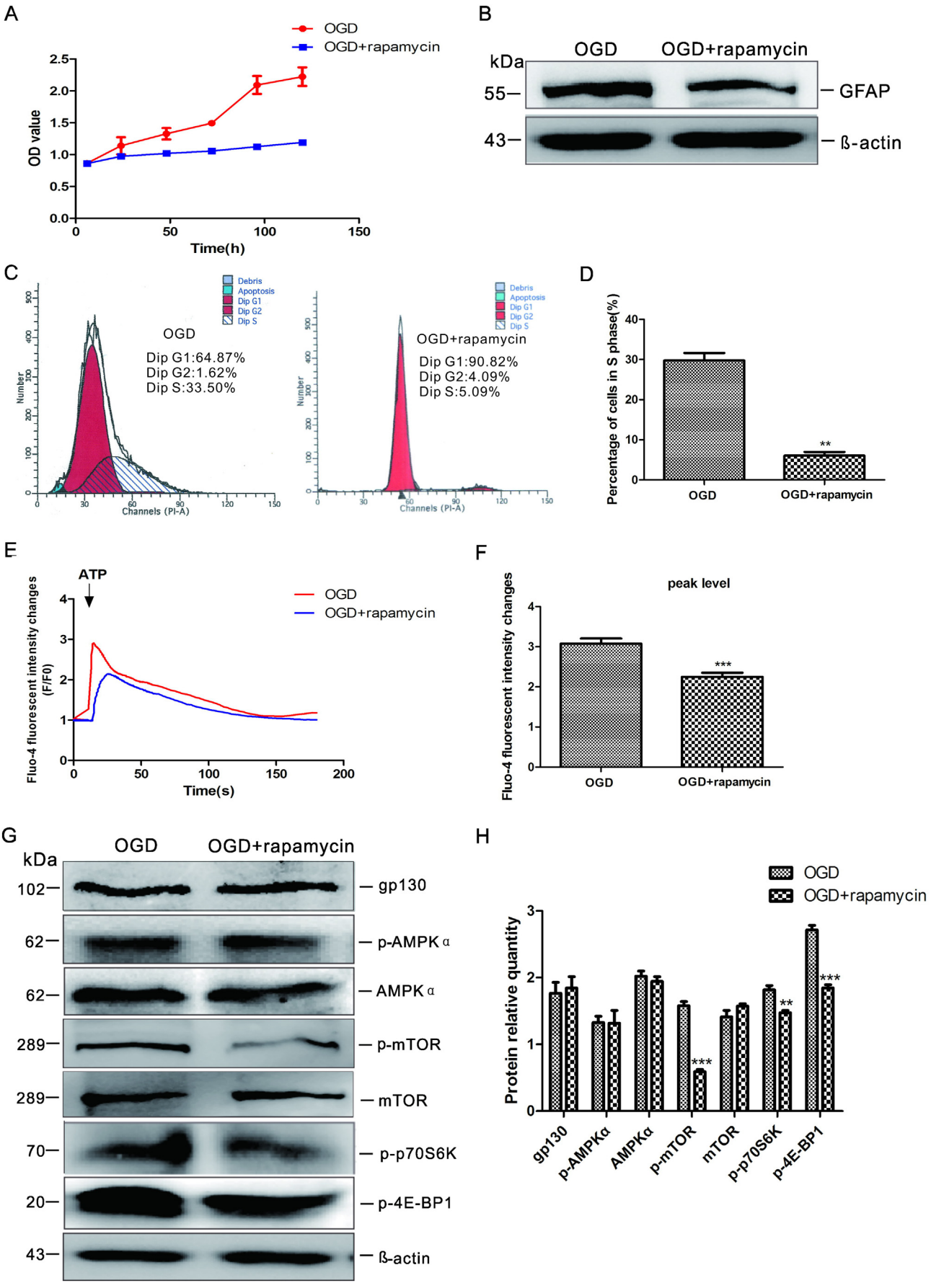

(caption on next page)

Fig. 10. Rapamycin represses the proliferation of OGD-injured astrocytes *in vitro* but does not affect the protein expression of gp130 and p-AMPKα. (A) Cell proliferation after OGD in the presence or absence of rapamycin treatment was detected within 6–120 h by CCK-8. (B) Representative western blot images of GFAP expression in the astrocytes of the two groups. (C) Representative images of the cell cycle in the OGD-injured astrocytes with or without rapamycin treatment as assessed by flow cytometry analysis. (D) The percentage change of astrocytes in the S phase in each group. (E) Changes in cytoplasmic Ca^{2+} ($[Ca^{2+}]_c$) in each group following ATP induction. (F) The peak values of the Fluo-4 fluorescence intensity of the two groups. (G-H) The expression levels of gp130, p-AMPKα, AMPKα, p-mTOR, mTOR, p-p7S6K and p-4E-BP1 were measured in the OGD-injured astrocytes with or without rapamycin treatment by western blotting and normalized to β-actin. Representative images are shown. The results are presented as the mean ± SEM. $^{**}P < 0.01$, $^{***}P < 0.001$. n = 3. n refers to the number of independent experiments.

induced increase in intracellular Ca^{2+} in the astrocytes injured by OGD. Therefore, we speculated that MSCs might regulate intracellular Ca^{2+} in astrocytes partially through the regulation of mTOR signaling to further modulate their proliferation.

In this study, we found that both MSCs transplantation and *in vitro* co-culture could facilitate IL-6 secretion in the injured microenvironment. Further use of siRNA technology displayed that siIL-6 MSCs transplantation could not suppress reactive astrocyte proliferation, which may result in the failure of functional recovery from HIBD. Conditional knockout of the signaling molecule signal transducer and activator of transcription 3 (STAT3) from astrocytes attenuated the upregulation of GFAP and caused astrocyte hypertrophy failure and a pronounced disruption of astroglial scar formation after spinal cord injury (Okada et al., 2006; Herrmann et al., 2008). In contrast, conditional deletion or functional knockdown of the signaling molecules suppressor of cytokine signaling 3 (SOCS3) or nuclear factor kappa-light-chain-enhancer of activated B cells (NF-κB) in astrocytes has been shown to reduce inflammation and lesion size after spinal cord injury or experimental autoimmune encephalomyelitis (EAE) (Okada et al., 2006; Brambilla et al., 2009). Therefore, reactive astrocytes exert diverse and complex functions in response to different forms of CNS damage or disease and can be regulated by different molecular signals in a context-specific manner. Our *in vitro* results indicated that the modulation of reactive astrocyte proliferation by MSCs is mediated by endogenous IL-6. Previous studies have confirmed that IL-6 can regulate AMPK in an exercise model (Kelly et al., 2004; Ruderman et al., 2006; Steinberg and Jørgensen, 2007). Furthermore, AMPK activation can reduce mTOR signaling (Inoki et al., 2012), which subsequently participates in the regulation of various astrocytic activities (Dello et al., 2009; Pastor et al., 2009; Wu et al., 2010; Dello et al., 2013). IL-6 can downregulate mTOR signaling, and application of AMPK inhibitors to C2C12 cells attenuated the inhibitory effect of IL-6 on mTOR (White et al., 2013). The present study revealed that through IL-6 secretion, MSCs upregulated the protein expression levels of gp130 and p-AMPKα but decreased the phosphorylation of mTOR and its downstream targets p70S6K and 4E-BP1 in OGD-injured astrocytes. p70S6K and 4E-BP1 in the mTOR signaling pathway mainly play important roles in protein translation and cell growth (Sabatini, 2006). Moreover, our results also suggested that there was a protein-protein interaction between gp130 and p-AMPKα. Consistent with the findings of other studies, these results indicated that rapamycin could effectively inhibit mTOR signaling induced by OGD injury and suppress reactive astrocyte proliferation (Li et al., 2015). AMPK/mTOR signaling has been confirmed to regulate the proliferation of various tumor cells, including glioma cells (Han et al., 2013; Jia et al., 2016; Zhao et al., 2017). Further study of the mTOR-specific inhibitor rapamycin has shown that suppression of mTOR signaling can improve learning and memory in HIBD rats, accompanied by a reduction in the proliferation of injured astrocytes *in vivo* and *in vitro*. It has been reported that inhibition of the mTOR pathway is required for neuroprotection in permanent MCAO (pMCAO) (Huang et al., 2014). Huang H showed that mTOR is a key endogenous neuroprotection mechanism in amyotrophic lateral sclerosis (ALS) (Saxena et al., 2013). The above findings suggest that MSCs suppress reactive astrocyte proliferation to improve the functional outcomes of HIBD injury, and this neuroprotective effect may involve the ability of endogenous IL-6 to activate the AMPK/mTOR signaling pathway through its receptor gp130. The mechanism by which gp130 regulates the AMPKα/mTOR signaling pathway and suppresses reactive proliferation will be the focus of our subsequent work.

5. Conclusions

In summary, this study confirmed that endogenous IL-6 secretion in response to MSCs transplantation indeed exerts neuroprotective functions on learning and memory in HIBD rats. A possible mechanism may be IL-6-induced activation of the AMPK/mTOR signaling pathway through gp130, which thereby downregulates reactive astrocyte proliferation to facilitate the maintenance of the normal biological functions of astrocytes. Thus, the above results imply that the therapeutic benefit of MSCs may originate from their accommodative role in the lesion microenvironment *via* immunomodulating reactive astrocytes at the subacute stage following HIBD.

Disclosure statement

The authors declare that they have no competing financial interests to disclose.

Acknowledgments

This work was supported by grants from the National Natural Science Foundation of China (81271385) and the Stem Cell Therapy for Special Study of Children's Hospital of Chongqing Medical University (SCT-201203).

MLH performed the research, analyzed the data and wrote the manuscript. XS and MY performed the experiments. TY provided advice on the experimental techniques. TYL provided the financial support. JC designed the experiments and provided the financial support. All authors read and approved the final manuscript.

References

Akkerman, S., Prickaerts, J., Steinbusch, H.W., Blokland, A., 2012. Object recognition testing: statistical considerations. Behav. Brain Res. 232, 317–322.
Anderson, M.F., Blomstrand, F., Blomstrand, C., Eriksson, P.S., Nilsson, M., 2003. Astrocytes and stroke: networking for survival. Neurochem. Res. 28, 293–305.
Aridas, J.D., Yawno, T., Sutherland, A.E., Nitsos, I., Ditchfield, M., Wong, F.Y., Fahey, M.C., Malhotra, A., Wallace, E.M., Jenkin, G., Miller, S.L., 2014. Detecting brain injury in neonatal hypoxic ischemic encephalopathy: closing the gap between experimental and clinical research. Exp. Neurol. 261, 281–290.
Barker, G.R., Warburton, E.C., 2011. When is the hippocampus involved in recognition memory. J. Neurosci. 31, 10721–10731.
Ben, S.I., Regazzetti, C., Robert, G., Laurent, K., Le, M.Y., Auberger, P., Tanti, J.F., Giorgetti-Peraldi, S., Bost, F., 2011. Metformin, independent of AMPK, induces mTOR inhibition and cell-cycle arrest through REDD1. Cancer Res. 71, 4366–4372.
Berridge, M.J., Lipp, P., Bootman, M.D., 2000. The versatility and universality of calcium signalling. Nat. Rev. Mol. Cell Biol. 1, 11–21.
Bi, Y., Gong, M., He, Y., Zhang, X., Zhou, X., Zhang, Y., Nan, G., Wei, X., Liu, Y., Chen, J., Li, T., 2014. AP2α transcriptional activity is essential for retinoid-induced neuronal differentiation of mesenchymal stem cells. Int. J. Biochem. Cell Biol. 46, 148–160.
Brambilla, R., Persaud, T., Hu, X., Karmally, S., Shestopalov, V.I., Dvoriantchikova, G., Ivanov, D., Nathanson, L., Barnum, S.R., Bethea, J.R., 2009. Transgenic inhibition of astroglial NF-kappa B improves functional outcome in experimental autoimmune encephalomyelitis by suppressing chronic central nervous system inflammation. J. Immunol. 182, 2628–2640.
Choudhury, G.R., Ding, S., 2016. Reactive astrocytes and therapeutic potential in focal ischemic stroke. Neurobiol. Dis. 85, 234–244.
Dazert, E., Hall, M.N., 2011. mTOR signaling in disease. Curr. Opin. Cell Biol. 23, 744–755.
Dello, R.C., Lisi, L., Tringali, G., Navarra, P., 2009. Involvement of mTOR kinase in

cytokine-dependent microglial activation and cell proliferation. Biochem. Pharmacol. 78, 1242–1251.
Dello, R.C., Lisi, L., Feinstein, D.L., Navarra, P., 2013. mTOR kinase, a key player in the regulation of glial functions: relevance for the therapy of multiple sclerosis. Glia 61, 301–311.
Donega, V., Nijboer, C.H., van Tilborg, G., Dijkhuizen, R.M., Kavelaars, A., Heijnen, C.J., 2014. Intranasally administered mesenchymal stem cells promote a regenerative niche for repair of neonatal ischemic brain injury. Exp. Neurol. 261, 53–64.
Faul, F., Erdfelder, E., Lang, A.G., Buchner, A., 2007. G*Power 3: a flexible statistical power analysis program for the social, behavioral, and biomedical sciences. Behav. Res. Methods 39, 175–191.
Florio, T., Grimaldi, M., Scorziello, A., Salmona, M., Bugiani, O., Tagliavini, F., Forloni, G., Schettini, G., 1996. Intracellular calcium rise through L-type calcium channels, as molecular mechanism for prion protein fragment 106-126-induced astroglial proliferation. Biochem. Biophys. Res. Commun. 228, 397–405.
Gadient, R.A., Otten, U.H., 1997. Interleukin-6 (IL-6)—a molecule with both beneficial and destructive potentials. Prog. Neurobiol. 52, 379–390.
Gao, Q., Katakowski, M., Chen, X., Li, Y., Chopp, M., 2005a. Human marrow stromal cells enhance connexin43 gap junction intercellular communication in cultured astrocytes. Cell Transplant. 14, 109–117.
Gao, Q., Li, Y., Chopp, M., 2005b. Bone marrow stromal cells increase astrocyte survival via upregulation of phosphoinositide 3-kinase/threonine protein kinase and mitogen-activated protein kinase kinase/extracellular signal-regulated kinase pathways and stimulate astrocyte trophic factor gene expression after anaerobic insult. Neuroscience 136, 123–134.
Gao, Q., Li, Y., Shen, L., Zhang, J., Zheng, X., Qu, R., Liu, Z., Chopp, M., 2008. Bone marrow stromal cells reduce ischemia-induced astrocytic activation in vitro. Neuroscience 152, 646–655.
Gong, M., Bi, Y., Jiang, W., Zhang, Y., Chen, L., Hou, N., Chen, J., Li, T., 2013. Retinoic acid receptor beta mediates all-trans retinoic acid facilitation of mesenchymal stem cells neuronal differentiation. Int. J. Biochem. Cell Biol. 45, 866–875.
Gu, Y., He, M., Zhou, X., Liu, J., Hou, N., Bin, T., Zhang, Y., Li, T., Chen, J., 2016. Endogenous IL-6 of mesenchymal stem cell improves behavioral outcome of hypoxic-ischemic brain damage neonatal rats by supressing apoptosis in astrocyte. Sci. Rep. 6, 18587.
Han, D., Li, S.J., Zhu, Y.T., Liu, L., Li, M.X., 2013. LKB1/AMPK/mTOR signaling pathway in non-small-cell lung cancer. Asian Pac. J. Cancer Prev. 14, 4033–4039.
He, M.L., Liu, J.J., Gu, Y., Li, T.Y., Chen, J., 2014. Effects of inhibiting secretion of mesenchymal stem cells originated interleukin-6 on oxygen glucose deprivation injured PC12 cells. J. Shanghai Jiao Tong Univ. Med. Sci. 34, 1435–1447.
Heinrich, P.C., Behrmann, I., Haan, S., Hermanns, H.M., Müller-Newen, G., Schaper, F., 2003. Principles of interleukin (IL)-6-type cytokine signalling and its regulation. Biochem. J. 374, 1–20.
Herrmann, J.E., Imura, T., Song, B., Qi, J., Ao, Y., Nguyen, T.K., Korsak, R.A., Takeda, K., Akira, S., Sofroniew, M.V., 2008. STAT3 is a critical regulator of astrogliosis and scar formation after spinal cord injury. J. Neurosci. 28, 7231–7243.
Hou, N., Ren, L., Gong, M., Bi, Y., Gu, Y., Dong, Z., Liu, Y., Chen, J., Li, T., 2015. Vitamin A deficiency impairs spatial learning and memory: the mechanism of abnormal CBP-dependent histone acetylation regulated by retinoic acid receptor alpha. Mol. Neurobiol. 51, 633–647.
Huang, H., Zhong, R., Xia, Z., Song, J., Feng, L., 2014. Neuroprotective effects of rhynchophylline against ischemic brain injury via regulation of the Akt/mTOR and TLRs signaling pathways. Molecules 19, 11196–11210.
Inoki, K., Kim, J., Guan, K.L., 2012. AMPK and mTOR in cellular energy homeostasis and drug targets. Annu. Rev. Pharmacol. Toxicol. 52, 381–400.
Ji, Y.F., Zhou, L., Xie, Y.J., Xu, S.M., Zhu, J., Teng, P., Shao, C.Y., Wang, Y., Luo, J.H., Shen, Y., 2013. Upregulation of glutamate transporter GLT-1 by mTOR-Akt-NF-κB cascade in astrocytic oxygen-glucose deprivation. Glia 61, 1959–1975.
Jia, Y., Wang, H., Wang, Q., Ding, H., Wu, H., Pan, H., 2016. Silencing Nrf2 impairs glioma cell proliferation via AMPK-activated mTOR inhibition. Biochem. Biophys. Res. Commun. 469, 665–671.
Kelly, M., Keller, C., Avilucea, P.R., Keller, P., Luo, Z., Xiang, X., Giralt, M., Hidalgo, J., Saha, A.K., Pedersen, B.K., Ruderman, N.B., 2004. AMPK activity is diminished in tissues of IL-6 knockout mice: the effect of exercise. Biochem. Biophys. Res. Commun. 320, 449–454.
Klann, E., Dever, T.E., 2004. Biochemical mechanisms for translational regulation in synaptic plasticity. Nat. Rev. Neurosci. 5, 931–942.
Laplante, M., Sabatini, D.M., 2012. mTOR signaling in growth control and disease. Cell 149, 274–293.
Li, Y., Chen, J., Zhang, C.L., Wang, L., Lu, D., Katakowski, M., Gao, Q., Shen, L.H., Zhang, J., Lu, M., Chopp, M., 2005. Gliosis and brain remodeling after treatment of stroke in rats with marrow stromal cells. Glia 49, 407–417.
Li, L., Lundkvist, A., Andersson, D., Wilhelmsson, U., Nagai, N., Pardo, A.C., Nodin, C., Ståhlberg, A., Aprico, K., Larsson, K., Yabe, T., Moons, L., Fotheringham, A., Davies, I., Carmeliet, P., Schwartz, J.P., Pekna, M., Kubista, M., Blomstrand, F., Maragakis, N., Nilsson, M., Pekny, M., 2008. Protective role of reactive astrocytes in brain ischemia. J. Cereb. Blood Flow Metab. 28, 468–481.
Li, X.L., Jia, T.M., Luan, B., Liu, T., Yuan, Y., 2011. Effects of electric stimulation at the cerebellar fastigial nucleus on astrocytes in the hippocampus of neonatal rats with hypoxic-ischemic brain damage. Zhongguo Dang Dai Er Ke Za Zhi 13, 317–320.
Li, C.Y., Li, X., Liu, S.F., Qu, W.S., Wang, W., Tian, D.S., 2015. Inhibition of mTOR pathway restrains astrocyte proliferation, migration and production of inflammatory mediators after oxygen-glucose deprivation and reoxygenation. Neurochem. Int. 83–84, 9–18.
Low, J.A., 2004. Determining the contribution of asphyxia to brain damage in the neonate. J. Obstet. Gynaecol. Res. 30, 276–286.
Madrigal, J.L., Dello, R.C., Gavrilyuk, V., Feinstein, D.L., 2006. Effects of noradrenaline on neuronal NOS2 expression and viability. Antioxid. Redox Signal. 8, 885–892.
Morris, R., 1984. Developments of a water-maze procedure for studying spatial learning in the rat. J. Neurosci. Methods 11, 47–60.
Ogawa, A., Firth, A.L., Yao, W., Madani, M.M., Kerr, K.M., Auger, W.R., Jamieson, S.W., Thistlethwaite, P.A., Yuan, J.X., 2009. Inhibition of mTOR attenuates store-operated Ca2+ entry in cells from endarterectomized tissues of patients with chronic thromboembolic pulmonary hypertension. Am. J. Phys. Lung Cell. Mol. Phys. 297, L666–L676.
Okada, S., Nakamura, M., Katoh, H., Miyao, T., Shimazaki, T., Ishii, K., Yamane, J., Yoshimura, A., Iwamoto, Y., Toyama, Y., Okano, H., 2006. Conditional ablation of Stat3 or Socs3 discloses a dual role for reactive astrocytes after spinal cord injury. Nat. Med. 12, 829–834.
Pastor, M.D., García-Yébenes, I., Fradejas, N., Pérez-Ortiz, J.M., Mora-Lee, S., Tranque, P., Moro, M.A., Pende, M., Calvo, S., 2009. mTOR/S6 kinase pathway contributes to astrocyte survival during ischemia. J. Biol. Chem. 284, 22067–22078.
Pekny, M., Nilsson, M., 2005. Astrocyte activation and reactive gliosis. Glia 50, 427–434.
Pekny, M., Pekna, M., 2014. Astrocyte reactivity and reactive astrogliosis: costs and benefits. Physiol. Rev. 94, 1077–1098.
Qu, R., Li, Y., Gao, Q., Shen, L., Zhang, J., Liu, Z., Chen, X., Chopp, M., 2007. Neurotrophic and growth factor gene expression profiling of mouse bone marrow stromal cells induced by ischemic brain extracts. Neuropathology 27, 355–363.
Rice, J.E., Vannucci, R.C., Brierley, J.B., 1981. The influence of immaturity on hypoxic-ischemic brain damage in the rat. Ann. Neurol. 9, 131–141.
Ruderman, N.B., Keller, C., Richard, A.M., Saha, A.K., Luo, Z., Xiang, X., Giralt, M., Ritov, V.B., Menshikova, E.V., Kelley, D.E., Hidalgo, J., Pedersen, B.K., Kelly, M., 2006. Interleukin-6 regulation of AMP-activated protein kinase. Potential role in the systemic response to exercise and prevention of the metabolic syndrome. Diabetes 55 (Suppl. 2), S48–S54.
Sabatini, D.M., 2006. mTOR and cancer: insights into a complex relationship. Nat. Rev. Cancer 6, 729–734.
Sabir, H., Scull-Brown, E., Liu, X., Thoresen, M., 2012. Immediate hypothermia is not neuroprotective after severe hypoxia-ischemia and is deleterious when delayed by 12 hours in neonatal rats. Stroke 43, 3364–3370.
Saxena, S., Roselli, F., Singh, K., Leptien, K., Julien, J.P., Gros-Louis, F., Caroni, P., 2013. Neuroprotection through excitability and mTOR required in ALS motoneurons to delay disease and extend survival. Neuron 80, 80–96.
Shankaran, S., Laptook, A., Wright, L.L., Ehrenkranz, R.A., Donovan, E.F., Fanaroff, A.A., Stark, A.R., Tyson, J.E., Poole, K., Carlo, W.A., Lemons, J.A., Oh, W., Stoll, B.J., Papile, L.A., Bauer, C.R., Stevenson, D.K., Korones, S.B., McDonald, S., 2002. Whole-body hypothermia for neonatal encephalopathy: animal observations as a basis for a randomized, controlled pilot study in term infants. Pediatrics 110, 377–385.
Sofroniew, M.V., 2009. Molecular dissection of reactive astrogliosis and glial scar formation. Trends Neurosci. 32, 638–647.
Steinberg, G.R., Jørgensen, S.B., 2007. The AMP-activated protein kinase: role in regulation of skeletal muscle metabolism and insulin sensitivity. Mini-Rev. Med. Chem. 7, 519–526.
Sukumari-Ramesh, S., Alleyne, C.H., Dhandapani, K.M., 2012. Astrogliosis: a target for intervention in intracerebral hemorrhage. Transl Stroke Res 3, 80–87.
Vannucci, S.J., Hagberg, H., 2004. Hypoxia-ischemia in the immature brain. J. Exp. Biol. 207, 3149–3154.
van Velthoven, C.T., Kavelaars, A., van Bel, F., Heijnen, C.J., 2010a. Repeated mesenchymal stem cell treatment after neonatal hypoxia-ischemia has distinct effects on formation and maturation of new neurons and oligodendrocytes leading to restoration of damage, corticospinal motor tract activity, and sensorimotor function. J. Neurosci. 30, 9603–9611.
van Velthoven, C.T., Kavelaars, A., van Bel, F., Heijnen, C.J., 2010b. Mesenchymal stem cell treatment after neonatal hypoxic-ischemic brain injury improves behavioral outcome and induces neuronal and oligodendrocyte regeneration. Brain Behav. Immun. 24, 387–393.
van Velthoven, C.T., Kavelaars, A., van Bel, F., Heijnen, C.J., 2010c. Nasal administration of stem cells: a promising novel route to treat neonatal ischemic brain damage. Pediatr. Res. 68, 419–422.
van Velthoven, C.T., Kavelaars, A., van Bel, F., Heijnen, C.J., 2011. Mesenchymal stem cell transplantation changes the gene expression profile of the neonatal ischemic brain. Brain Behav. Immun. 25, 1342–1348.
Verkhratsky, A., Sofroniew, M.V., Messing, A., Delanerolle, N.C., Rempe, D., Rodríguez, J.J., Nedergaard, M., 2012. Neurological diseases as primary gliopathies: a re-assessment of neurocentrism. ASN Neuro 4.
van Vliet, E.A., Forte, G., Holtman, L., den Burger, J.C., Sinjewel, A., de Vries, H.E., Aronica, E., Gorter, J.A., 2012. Inhibition of mammalian target of rapamycin reduces epileptogenesis and blood-brain barrier leakage but not microglia activation. Epilepsia 53, 1254–1263.
Wang, R., Zhang, X., Zhang, J., Fan, Y., Shen, Y., Hu, W., Chen, Z., 2012. Oxygen-glucose deprivation induced glial scar-like change in astrocytes. PLoS One 7, e37574.
Wanner, I.B., Deik, A., Torres, M., Rosendahl, A., Neary, J.T., Lemmon, V.P., Bixby, J.L., 2008. A new in vitro model of the glial scar inhibits axon growth. Glia 56, 1691–1709.
White, J.P., Puppa, M.J., Gao, S., Sato, S., Welle, S.L., Carson, J.A., 2013. Muscle mTORC1 suppression by IL-6 during cancer cachexia: a role for AMPK. Am. J. Physiol. Endocrinol. Metab. 304, E1042–E1052.
Winder, W.W., 2001. Energy-sensing and signaling by AMP-activated protein kinase in skeletal muscle. J. Appl. Physiol. 91, 1017–1028.
Wu, X., Kihara, T., Akaike, A., Niidome, T., Sugimoto, H., 2010. PI3K/Akt/mTOR signaling regulates glutamate transporter 1 in astrocytes. Biochem. Biophys. Res. Commun. 393, 514–518.

Yasuhara, T., Matsukawa, N., Yu, G., Xu, L., Mays, R.W., Kovach, J., Deans, R.J., Hess, D.C., Carroll, J.E., Borlongan, C.V., 2006. Behavioral and histological characterization of intrahippocampal grafts of human bone marrow-derived multipotent progenitor cells in neonatal rats with hypoxic-ischemic injury. Cell Transplant. 15, 231–238.

Yenari, M., Kitagawa, K., Lyden, P., Perez-Pinzon, M., 2008. Metabolic downregulation: a key to successful neuroprotection? Stroke; a journal of cerebral circulation. Stroke 39, 2910–2917.

Zamanian, J.L., Xu, L., Foo, L.C., Nouri, N., Zhou, L., Giffard, R.G., Barres, B.A., 2012. Genomic analysis of reactive astrogliosis. J. Neurosci. 32, 6391–6410.

Zhao, K., Wang, L., Li, T., Zhu, M., Zhang, C., Chen, L., Zhao, P., Zhou, H., Yu, S., Yang, X., 2017. The role of miR-451 in the switching between proliferation and migration in malignant glioma cells: AMPK signaling, mTOR modulation and Rac1 activation required. Int. J. Oncol. 50, 1989–1999.

Zhou, X., Gu, J., Gu, Y., He, M., Bi, Y., Chen, J., Li, T., 2015. Human umbilical cord-derived mesenchymal stem cells improve learning and memory function in hypoxic-ischemic brain-damaged rats via an IL-8-mediated secretion mechanism rather than differentiation pattern induction. Cell. Physiol. Biochem. 35, 2383–2401.

Zhu, H., Jiang, L., Qiao, L.X., Huang, L., Zhu, L.H., Zhang, Z.H., 2007a. Observation on hippocampus proliferation following hypoxic-ischemic brain damage in neonatal rats. J. Southeast Univ. 26, 177–180.

Zhu, Z., Zhang, Q., Yu, Z., Zhang, L., Tian, D., Zhu, S., Bu, B., Xie, M., Wang, W., 2007b. Inhibiting cell cycle progression reduces reactive astrogliosis initiated by scratch injury in vitro and by cerebral ischemia in vivo. Glia 55, 546–558.